CHEMISTRY OF MATERIALS
Cite This: Chem. Mater. 2018, 30, 5799−5813
Perspective
pubs.acs.org/cm

Germanium Chalcogenide Thermoelectrics: Electronic Structure Modulation and Low Lattice Thermal Conductivity†

Subhajit Roychowdhury,‡ Manisha Samanta,‡ Suresh Perumal,‡ and Kanishka Biswas*,‡,§

‡New Chemistry Unit, Jawaharlal Nehru Centre for Advanced Scientific Research (JNCASR), Jakkur P.O., Bangalore 560064, India
§School of Advanced Materials (SAMat), Jawaharlal Nehru Centre for Advanced Scientific Research (JNCASR), Jakkur P.O., Bangalore 560064, India

ABSTRACT: Thermoelectric materials can convert untapped heat to electricity and are expected to have an important role in future energy utilization. IV−VI metal chalcogenides are the most promising candidates for mid-temperature thermoelectric power generation. Among them, PbTe and their alloys have been proven to be the superior thermoelectric materials. Unfortunately, the toxicity of lead (Pb) prevents the application of lead chalcogenides and demands the search for lead-free high-performance solids. This perspective discusses the recent progress of thermoelectric property studies on germanium chalcogenides (GeTe, GeSe, and GeS) for mid-temperature power generation. Here, we have discussed the crystal structure, chemical bonding, and phonon dispersion of germanium chalcogenides to understand the underlying lattice dynamics and low lattice thermal conductivity from a chemistry perspective. We have also discussed the uniqueness of the electronic structure of GeTe and GeSe, which plays an important role in tailoring thermoelectric properties. Additionally, the implications of the recent state-of-art strategies such as resonant level formation, valence band convergence, slight symmetry breaking of the crystal and electronic structures, point defect, and nanostructure induced phonon scattering on the high thermoelectric performance of the germanium chalcogenides are discussed in detail. In conclusion, we highlight some of the innovative ideas for discovery and designing of new thermoelectric compositions. Finally, we point out the major challenges and opportunities in this field. All the strategies discussed in this perspective not only make germanium chalcogenides as a promising candidate for future thermoelectric applications but also serve as a guide to enhance the thermoelectric performance of other materials.

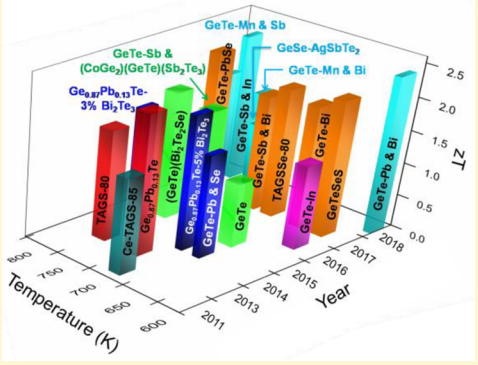

INTRODUCTION

Thermoelectric technology, devoid of any moving parts, can directly convert waste heat into electrical power without any hazardous greenhouse gas emission.[1−4] From the materials perspective, the thermoelectric conversion efficiency is limited by the dimensionless figure of merit, $zT = \sigma S^2 T/(\kappa_{el} + \kappa_{lat})$, where, σ, S, T, κ_{el}, and κ_{lat} are electrical conductivity, Seebeck coefficient, absolute temperature, electrical thermal conductivity, and lattice thermal conductivity, respectively.[1−5] An ideal thermoelectric material should have high electrical conductivity similar to metals, large Seebeck coefficient as in semiconductors, and ultralow thermal conductivity like glasses.[1] However, it is always challenging for the chemists to combine all these aspects in a single material to enable high thermoelectric performance. In the past two decades, several endeavors have been made to decouple the interdependent parameters and simultaneously enhance the thermoelectric performances.[1,2] zT of materials can be enhanced simultaneously by improving the power factor (σS^2) via introducing resonant states close to the Fermi level in the electronic structure,[6,7] convergence of valence/conduction band valleys,[8−10] carrier energy filtering,[11] and quantum confinement,[12] and by reducing the lattice thermal conductivity (κ_{lat}) via introduction of hierarchical nano-/meso-architectures[13−17] or by intrinsic factors,[18] which scatter all length-scale heat carrying phonons.

Lead chalcogenides have been broadly contemplated as the leading materials in mid-temperature (600−900 K) thermoelectric power generation.[8,13,14,19] Unfortunately, the toxicity of lead (Pb) prevents the mass-market application of lead chalcogenides and demands the search for lead-free high-performance material. Germanium chalcogenides (GeTe, GeSe, and GeS) from the IV−VI family recently emerged as potential candidates for the replacement of Pb-based chalcogenides.[16,20−22] The thermoelectric efficiency of pristine GeTe is limited by high *p*-type carrier concentration, resulting from intrinsic Ge vacancies.[22] Whereas, the poor electrical conductivity with low carrier concentration is mainly responsible for poor TE performance of GeSe and GeS which needs further optimization.[23−25] Recently, GeTe has been widely studied for thermoelectrics because of their rich

†This Perspective is part of the *Up-and-Coming* series.

Received: June 25, 2018
Revised: August 6, 2018
Published: August 7, 2018

DOI: 10.1021/acs.chemmater.8b02676
Chem. Mater. 2018, 30, 5799−5813

structural chemistry and electronic structure.[22] GeTe undergoes structural phase transition from room temperature rhombohedral phase (low symmetry, *R*3*m*, ferroelectric) to high-temperature cubic phase (high symmetry, $Fm\bar{3}m$, paraelectric) without changing the number of atoms in the unit cell at 700 K.[26] The ferroelectric phase transition is identified by softening of transverse optical (TO) phonon modes at the zone center (Γ).[26] This displacive phase transition in GeTe has been further confirmed by Raman scattering and density functional theory (DFT) calculations.[27−29]

Tracing back the strategies for the enhancement of TE materials, the high carrier concentration of GeTe has been optimized by substitution of the group-15 elements (Sb/Bi).[20,30] Recently, In doping created a resonant level near the valence band of GeTe that enhanced the Seebeck coefficient similar to In-doped SnTe.[7,31] Moreover, Sb/Bi decreases the lattice thermal conductivity due to formation of nano-/mesostructures.[20,30] Thus, codoping of In and Sb or Sb and Bi is proven to be an effective strategy for the enhancement of TE performance throughout the measured temperature range.[32,33] To achieve the goal of simultaneous carrier and phonon engineering, GeTe has been broadly alloyed with I−V−VI_2 material such as $AgSbTe_2$ and $AgSbSe_2$ (known as TAGS and TAGSSe, respectively) which resulted in a high zT_{max} of ∼1.9 at 660 K for the $(GeTe)_{80}(AgSbSe_2)_{20}$ sample with a high average zT (zT_{avg}) of ∼1.4 in the temperature range of 300−700 K.[21,34−36] Although TAGS based materials are well-known as they are being used as the *p*-type leg in radio-isotope thermoelectric generators in NASA,[37] GeTe is still far away from the goal of replacing high-performance PbTe. Gelbstein and co-workers have achieved a high zT of ∼2.2 at 723 K in GeTe via alloying with Pb.[38,39] The solubility of Pb in the GeTe matrix is further enhanced by adding 3 mol % of Bi_2Te_3 which decreases lattice thermal conductivity owing to excessive point defect scattering.[40] Recently, a high zT of ∼2.1 at 630 K has been observed for $(GeTe)_{1-2x}(GeSe)_x(GeS)_x$ due to the ultralow thermal conductivity, resulting from the entropy-driven point defect scattering.[16]

Since 1960, the main focus is on the improvement of TE performance of high-temperature cubic phase of GeTe similar to PbTe or SnTe, whereas GeTe is the only metal telluride in the IV−VI semiconductor family which crystallizes in the rhombohedral structure at room temperature.[22] Rhombohedral distortion in GeTe splits 4 equivalent L bands and 12 Σ bands of cubic GeTe into (3 L and 1 Z) and (6 Σ + 6 η) bands of rhombohedral GeTe in the Brillouin Zone which is not much favorable for the band convergence in the rhombohedral phase.[34] Recently, Li et al. have obtained unprecedented high zT of ∼2.4 at 600 K with a record high device figure of merit, ZT ∼ 1.5, in rhombohedral GeTe by introducing slight symmetry reduction from cubic to rhombohedral structure via Bi doping.[41,42]

Recently, the discovery of an unprecedented high thermoelectric figure of merit (zT) of ∼2.6 in SnSe has drawn attention to study other lead-free layered two-dimensional chalcogenides from the IV−VI family.[43] At ambient conditions, GeSe has a layered crystal structure (space group *Pnma*) similar to that of SnSe.[23] Based on temperature and pressure, GeSe crystallizes in three dissimilar crystal structures, namely, orthorhombic (space group, *Pnma*), rhombohedral (space group, *R*3*m*), and cubic (space group, $Fm\bar{3}m$). Whereas, GeS undergoes a structural phase transition from *Pnma* to high symmetric *Cmcm* phase at ∼863 K.[25] In Figure 1, we have summarized the potential germanium chalcogenide based thermoelectric materials with their zT's and the year of discovery.

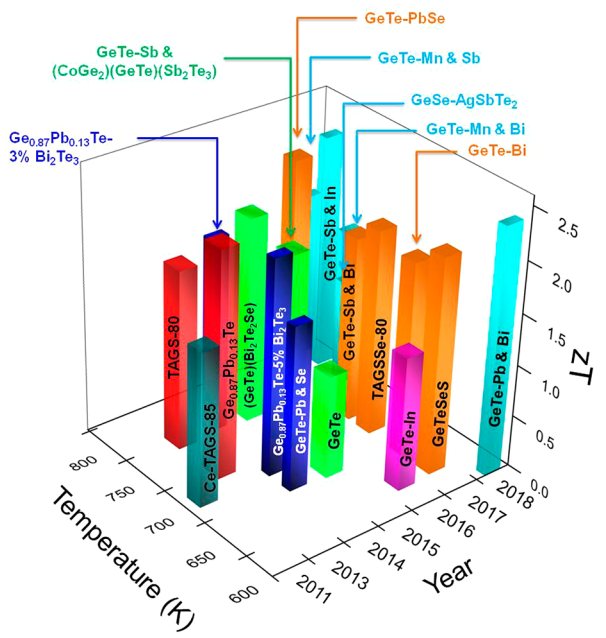

Figure 1. Thermoelectric figure of merit, zT, as a function of temperature and year representing the major milestone in the germanium chalcogenide research.

Here, we have discussed the recent progress and challenges on the enhancement of thermoelectric properties of germanium chalcogenides by using state-of-the-art approaches. This perspective will motivate researchers to further investigate and improve the performance of germanium chalcogenides to replace the lead-based materials for the mass-market applications. The perspective is arranged as follows: first, we briefly summarized the chemical bonding, crystal structure, and phonon dispersion of GeTe. Then, we discussed the enhancement of the Seebeck coefficient by using electronic structure modulation such as the formation of resonance state, convergence of the valence band valleys, and the newly discovered slight symmetry reduction in GeTe. The discussion is followed by the mechanism of the reduction of lattice thermal conductivity by alloying and nanostructuring approaches. Next, we have mentioned the progress of layered germanium chalcogenides (GeSe and GeS) as effective *p*-type thermoelectric materials. Finally, we conclude by providing possible directions and challenges for further improvement of TE performance of technologically important germanium chalcogenide system.

CRYSTAL STRUCTURE AND LATTICE DYNAMICS IN GeTe

In order to gain a better insight into the role of lattice dynamics on the thermal conductivity and other related properties of GeTe, it is essential to understand more about the chemical bonding, crystal structure, and phase transition of GeTe. GeTe has rocksalt crystal structure (space group $Fm\bar{3}m$ with a lattice constant of a = 6.009 Å), similar to lead chalcogenides (PbX; X = S, Se, Te) only at high temperature

DOI: 10.1021/acs.chemmater.8b02676
Chem. Mater. 2018, 30, 5799−5813

(>700 K).[44−46] Below 700 K, GeTe undergoes a structural distortion along the [111] direction of cubic structure and adopts rhombohedral structure ($R3m$ with the lattice parameters of $a = b = 4.164$ Å and $c = 10.690$ Å) (Figure 2).[22] Although similar structural distortion is also observed in

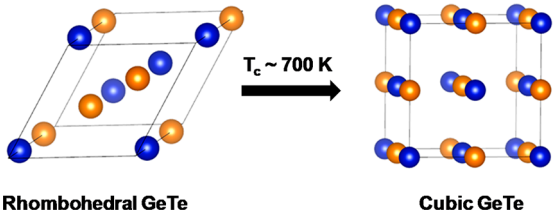

Figure 2. Rhombohedral to cubic structural phase transition in GeTe (blue and yellow atoms are Ge and Te, respectively).

semimetal Sb and Bi, GeTe is ferroelectric because of the presence of two different atoms (Ge and Te) with different electronegativities making the bonding polar.[44] At room temperature, the crystal structure of PbTe and SnTe is cubic, whereas GeTe crystallizes in the less symmetric rhombohedral crystal structure. This anomaly mainly governs by the presence of the ns^2 lone pair on the cation.[47] The role of the lone pair has long been invoked for explaining the off-centering structural distortion. The ns^2 lone pair can be either stereochemically active or quenched depending on the local bonding. Interestingly, as the molecular weight of the metal increases, the chance of quenching of the ns^2 lone pair increases, which favors the formation of high symmetry structure that is clearly seen in cubic SnTe and PbTe.[47] When comparing the orbital energy levels of GeTe and PbTe, the separation between the cation s and anion p electronic band is higher in PbTe than that of GeTe (see Figure 3),

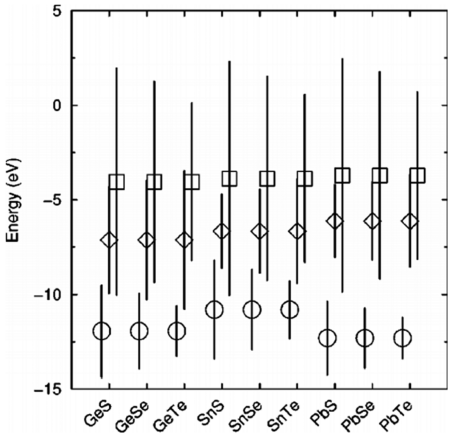

Figure 3. Atomic orbital energy and bandwidth of cation s (circle) and p bands (square) and anion p band (diamond) for IV−VI chalcogenides.[48] Reproduced with permission from ref 48. Copyright 2003, American Physical Society.

resulting in weak cation-s and anion-p interaction for PbTe (relativistic effect) which favors the stable rocksalt structure in PbTe, whereas GeTe undergoes a rhombohedral distortion.[47,48] GeTe is metallic, but other germanium chalcogenides such as GeS and GeS are a semiconductor.[22,24] This can be attributed to the better mixing of anion p and cation p orbitals in GeTe as the electronegativity decreases down the group in chalcogens (S to Te).[48]

The relative displacement of the Ge and Te sublattice along the [111] direction makes GeTe ferroelectric near room temperature. This distortion changes the angle $\alpha = 88.35°$ from ideal angle of 90° between the axes in the face-centered cubic unit cell.[20] The crystal structure turns noncentrosymmetric due to the atomic rearrangement, resulting in a spontaneous polarization of ~60 $\mu C/m^2$.[29,49] The similar structural phase transition has been realized previously in SnTe,[50] $Pb_{1-x}Ge_xTe$,[51] and $Pb_{1-x}Sn_xTe$[52] in low temperatures. The neutron diffraction study by Chattopadhyay et al. showed that this ferroelectric structural transition is displacive in nature.[26] Mention must be made that number of atoms (two) and formula unit (one) per primitive unit cell of GeTe for both the phases are same.[26] Moreover, density functional theory (DFT) calculation has indicated that this transition is mainly because of the displacement of Ge and Te.[46] However, recent local structural analysis by extended X-ray absorption fine structure (EXAFS) and pair distribution functional (PDF) have verified the ferroelectric structural transition is the order−disorder type.[53,54]

GeTe has gained much attention from both the researchers and industry because of its unique properties. Change in the microscopic structure from crystalline to amorphous phase is observed after Sb substitution.[55,56] Due to the fascinating properties such as ferroelectric and phase change behavior, GeTe becomes the heart of many experimental and theoretical studies. The ferroelectric phase transition in GeTe is identified by softening of transverse optical (TO) phonon modes at zone-center (Γ).[27] Raman scattering on GeTe showed the presence of two peaks at 98 and 140 cm^{-1} corresponding to E and A_1 modes, respectively, which arise due to the vibration of Ge and Te sublattices along and perpendicular to the 3-fold axis.[27] Softening of these two modes has been observed with increasing temperature.[27,46]

Recently, Wdowik et al. provide clear insight into the lattice dynamics of GeTe (both the phases α and β) together with inelastic neutron scattering experiments and density functional theory calculation.[29] To understand the thermal transport of both rhombohedral and cubic GeTe, it is important to examine phonon dispersions of both the phases. Phonon dispersion for α-GeTe at the Γ point exhibits six vibrational modes, namely, three acoustic modes, two transverse optical modes (TO), and one longitudinal optical mode (LO) (Figure 4a). Both A_1 (nondegenerate) and E (doubly degenerate) modes for rhombohedral GeTe (α-GeTe) are Raman and IR active owing to the absence of inversion symmetry in the structure. Whereas, phonon-dispersion of the high-symmetry rocksalt structure of GeTe (β phase) provide the evidence for the presence of several soft phonon modes, mainly TO components which are responsible for the symmetry change at the phase transition (Figure 4b).[29] Notably, phonon dispersion of cubic GeTe exhibits several imaginary modes in the Brillouin zone which is one of the reasons for the absence of cubic GeTe at ambient condition, whereas the rhombohedral phase exhibits real modes. The β phase exhibits local distortions similar to Peierls distortion, which result in three shorter (2.86 Å) and three longer (3.25 Å) Ge−Te bonds.[57,58]

Generalized phonon density of states displays the extension of the acoustic band is from 0 to ~11 eV.[29] The mixed vibration of the Ge and Te sublattice contributes to the acoustic and intermediate TO modes. The highest frequency region, composed of the LO-phonon band, is governed by the vibrations of the Ge sublattice, which is also confirmed by the

DOI: 10.1021/acs.chemmater.8b02676
Chem. Mater. 2018, 30, 5799−5813

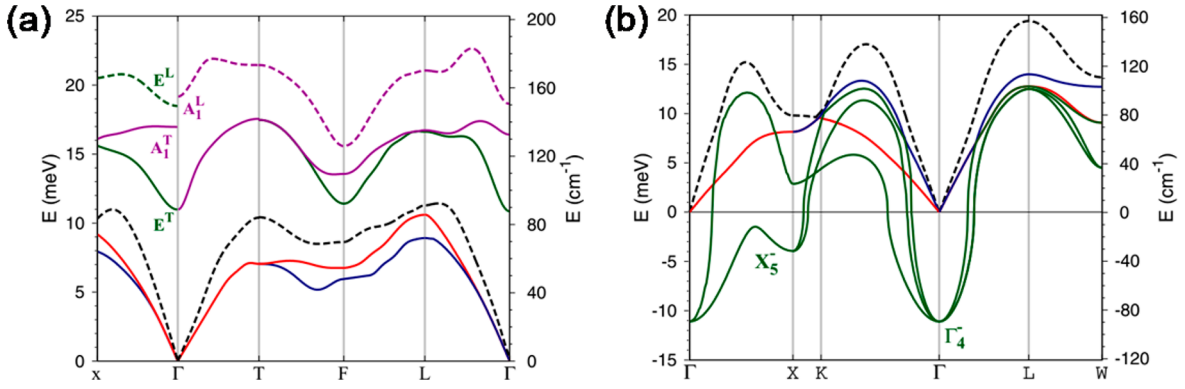

Figure 4. Phonon dispersion plot of (a) rhombohedral and (b) cubic GeTe. Solid and dashed lines represent transverse (T) and longitudinal (L) modes, respectively.[29] Reproduced with permission from ref 29. Copyright 2014, American Physical Society.

phonon density of state (Ph-DOS) calculation and the ^{125}Te nuclear inelastic scattering experiments.[59] Phonon DOS of cubic GeTe shows noticeable red-shift corresponding to rhombohedral GeTe which can be attributed to the phonon softening in the cubic phase.[32]

The high zT of a material demands low lattice thermal conductivity, κ_{lat}. Introduction of micro- and nanostructures in the matrix is the well-known approach to controlling the phonon propagation and hence thermal conductivity.[1,17] However, it is essential to understand the influence of chemical bonds on the phonon transport. Room temperature κ_{lat} for GeTe is ~2.7 W m^{-1} K^{-1} whereas for InSb is 16 W m^{-1} K^{-1}.[22,60] Although the structures of GeTe and InSb are different, according to simple mass disorder rule, they should follow the reverse trend as discussed previously by Lee et al.[60] Here, chemical bonding plays an important role. Softer bonding in GeTe compared to InSb leads to decrease in the speed of sound and the lattice thermal conductivity (eq 1):

$$\kappa_{lat} = \frac{1}{3} C_v \nu_a l \tag{1}$$

where, C_v, ν_a, and l are heat capacity at constant volume, sound velocity, and mean free path, respectively. Octahedral coordination in GeTe results in softer bonding compared to that of InSb (tetrahedral bonding) which leads to the decrease in the average sound velocity in GeTe (1900 m/s)[59] compared to InSb (2300 m/s)[61] and thereby lower lattice thermal conductivity in GeTe. Moreover, the presence of the soft transverse optical mode in GeTe[27,29,49] results in the reduced phonon mean free path (~1−100 nm for GeTe,[32] ~10−1000 nm for InSb[60]) which further favors achieving lower lattice thermal conductivity in GeTe compared to that of InSb. This soft-phonon mode mediated phase transition temperature can be decreased to room temperature from 700 K through proper carrier engineering, which can bring down the lattice thermal conductivity of GeTe to its minimum value and, thus, can improve the thermoelectric performance of GeTe near room temperature.

■ ELECTRONIC PROPERTIES

Electronic Structure of GeTe. The power factor ($S^2\sigma$) is a product of electrical conductivity (σ) and square of the Seebeck coefficient (S), which generally have an inverse relation to each other for the typical degenerate semiconductors as per the following equations,[37,62]

$$S = \frac{8^2\pi^2 k_B^{\ 2}}{3eh^2} m^* T \left[\frac{\pi}{3n}\right]^{2/3} \tag{2}$$

$$\sigma = ne\mu \tag{3}$$

$$S^2\sigma \propto \frac{N_V C_l}{m_I^* E_{def}^2} T \tag{4}$$

where k_B is the Boltzmann constant, e the electron charge, h the Planck constant, m^* the effective mass of carriers, n the carrier concentration, μ the carriers mobility, C_l the average longitudinal elastic moduli, m_I^* the inertial effective mass, N_V the total valley degeneracy, and E_{def} the deformation potential coefficient. From the above equations, it is clear that S and n have an inverse relation to one another, whereas σ is directly proportional to n. Equation 4 shows that the power factor ($S^2\sigma$), where acoustic phonon scattering dominates, is strongly depended on valley degeneracy (N_V) and inertial effective mass (m_I^*).[62] Thus, engineering the electronic structure with the appropriate dopants should be an essential route to increase the power factor via essentially the enhancement of the Seebeck coefficient. Further, uniform doping or alloying can significantly alter the electrical conductivity and enhance the Seebeck coefficient; however, the mobility would be strongly affected in this process. Thus, to enhance the Seebeck coefficient, many strategies have been employed, mainly by distorting the electronic structure such as valence and/or conduction sub-bands convergence, formation of resonant state at and around the Fermi level (E_F), and energy filtering where low energy minority carriers get blocked. IV−VI tellurides have two valence bands, the light hole valence band at L and the heavy hole valence band at the Σ point of the Brillouin zone. The energy separations between these two valence bands ($\Delta E_{L-\Sigma}$) are ~0.15 eV for PbTe[63,64] and ~0.35 for SnTe.[65,66] The increase in temperature and introduction of doping reduce the energy separation, which provides a path to access the heavy hole Σ-band for charge transport.[8,9,67]

GeTe adopts both rhombohedral ($R3m$) and cubic rock-salt structure ($Fm\bar{3}m$) at 300 K and above 700 K, respectively.[20] GeTe exhibits a theoretical principle band gap, E_g value of ~0.243 eV (experimental value being E_g ~ 0.21 eV). The valence band (VB) is formed by Te 5p states due to higher electronegativity of Te (χ_{Te} = 2.10) than that of Ge (χ_{Ge} = 2.01) and conduction band (CB) constituted by mainly Ge 4p states. The p-type narrow band gap GeTe exhibits low Seebeck coefficient (S ~ 34 μV/K), high electrical conductivity (σ ~ 8000 S/cm) due to large carrier density (10^{20}−10^{21} cm^{-3}), and

DOI: 10.1021/acs.chemmater.8b02676
Chem. Mater. 2018, 30, 5799−5813

large total thermal conductivity (κ_{total} ~ 8 W/(m·K)), which leads to zT of ~0.8 at 720 K.[20,68] Thus, suppressing the intrinsic Ge vacancies along with excess *p*-type carrier concentration significantly enhances the power factor through enhancement in the Seebeck coefficient ($S \propto (1/n)^{2/3}$).[37] The review article on GeTe published few years back has intensively summarized the suitable dopant elements and compounds that are capable of optimizing the carrier concentration and thermoelectric properties.[22] In this perspective, we have mainly focused on chemical bonding, modulation of electronic/phonon structures, recent trends, and newly implemented strategies in order to improve the thermoelectric properties of not only GeTe but also other important Ge-chalcogenides.

Electronic Band Convergence. Effect of valence band convergence has been realized in GeTe based systems as it has two valence bands, light hole valence band (L point, effective mass of $1.3m_0$) and heavy hole valence band (Σ point, effective mass of $6.1m_0$)[40] (Figure 5a,b) with energy separation ($\Delta E_{L-\Sigma}$) of ~0.27−0.38 eV in its cubic phase (Figure 5b).[69−72] Recently Wu et al.[40] have found that 3 mol % of Bi_2Te_3 doped $Ge_{0.87}Pb_{0.13}Te$ showed a large Seebeck value of 273 μV/K at 773 K (Figure 5c), which led to zT of 1.9 at 773 K, and the obtained high *S* values were clearly situated far above the Pisarenko line (*S* vs *n*) at 623 K (Figure 5d). To understand the reason behind the enhancement of the Seebeck coefficient, electronic structure calculations have been carried out which clearly revealed that the energy offset of ~0.23 eV between two valence bands decreases to ~0.14 eV (Figure 5e) that facilitates valence band convergence in 3 mol % of Bi_2Te_3 doped $Ge_{0.87}Pb_{0.13}Te$.[40] Charge carriers of heavy Σ-band contribute to conduction, thereby enhancing the Seebeck coefficient without degrading electrical conductivity. The schematic diagram of valence band convergence that was realized in GeTe is illustrated in Figure 5f. The 3 mol % Bi_2Te_3 addition of GeTe increases the solubility of Pb, which enhances valence band convergence by decreasing the extent of rhombohedral distortion in cubic GeTe. Further, Sb doping GeTe has shown a high zT of 1.85 at 700 K due to the observed large *S* value of 256 μV/K at 723 K (Figure 5c). Aliovalent Sb^{3+} doping at the Ge^{2+} site in GeTe effectively suppressed *p*-type carrier density, and Sb doping increases the valley degeneracy (N_V ~ 12) as the addition of Sb promotes the system to be more in cubic ($Fm\bar{3}m$) structure rather than rhombohedral ($R3m$), thereby enhancing the Seebeck coefficient.[20,68] The *S* values of $Ge_{0.9}Sb_{0.1}Te$ were also not following the Pisarenko line, and it showed higher effective mass (m^*) of 2.07 m_0 than that of the pristine GeTe (1.43 m_0). Both the reductions in *p*-type carrier density and increase in valley degeneracy have accounted for enhancement of *S* values upon Sb doping in GeTe. To have further insights on the role of Sb in GeTe, electronic structure calculations using DFT were performed which revealed that substitution of Sb in GeTe reduces the energy separation ($\Delta E_{L-\Sigma}$) between light L and heavy Σ bands, from ~0.21 eV for GeTe to ~0.16 eV for $Ge_{14}Sb_2Te_{16}$, which indicates a move toward valence band convergence.[33] Moreover, Bi and Sb codoped GeTe decreases the energy offset value further down to ~0.15 eV for $Ge_{13}BiSb_2Te_{16}$, which led to the high zT of ~1.8 at 725 K.[33]

Recently, Zheng et al.[73] have shown that alloying of MnTe in GeTe effectively reduces the energy difference between light and heavy hole valence bands, which enhances the valence band convergence. As the MnTe concentration increases in GeTe the energy offset ($\Delta E_{L-\Sigma}$) between L and Σ bands decreases from ~0.21 eV for GeTe to ~0.05 eV and ~0.01 eV for $Ge_{26}MnTe_{27}$ and $Ge_{25}Mn_2Te_{16}$, respectively. The calculated effective mass of charge carries in $Ge_{0.85}Mn_{0.15}Te$ is ~4.69 m_0, which is notably higher as compared to pure GeTe (~1.44 m_0), which suggests that the second/heavy valence band participates in conduction via valence band convergence and subsequently enhances the Seebeck coefficient upon Mn doping in GeTe.[73] It is to be noted that the measured Seebeck values do not fit the Pisarenko line using a simple parabolic single band model and even a two-band model (Figure 5d). However, Mn substituted GeTe samples have not shown much improvement in zT due to the obtained low power factor and considerably high thermal conductivity. Thus, the carrier concentration of $Ge_{1-x}Mn_xTe$ was optimized by substitution of Sb in GeTe. Due to the strong aliovalent nature of Sb, the carrier concentration was reduced from 2.25 × 10^{21} cm^{-3} to 8.37 × 10^{20} cm^{-3} for $Ge_{0.90}Mn_{0.10}Te$ to $Ge_{0.82}Mn_{0.10}Sb_{0.08}Te$, respectively. With the addition to the Seebeck coefficient, the power factor was significantly increased and the maximum power factor of ~30 μW cm^{-1} K^{-2} at 673 K was obtained for the composition of $Ge_{0.84}Mn_{0.10}Sb_{0.06}Te$. A maximum zT of

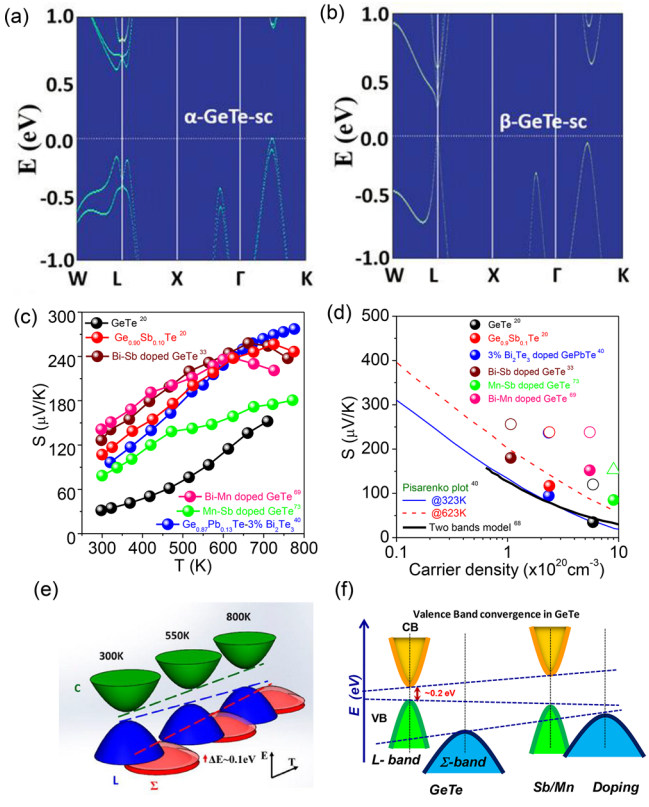

Figure 5. Electronic structure of (a) rhombohedral (α phase) and (b) cubic (β phase) GeTe.[69] (c) Temperature dependent Seebeck coefficient (*S*) of GeTe based materials. (d) Seebeck coefficient vs carrier concentration plot for various GeTe samples at 300 and 623 K. Solid and dotted lines represent the theoretical Pisarenko plot of GeTe at 300 and 623 K, respectively.[40] (e) Schematic illustration of the band offsets among the L, Σ, and C bands with temperature.[40] (f) Schematic electronic structure of GeTe and $Ge_{1-x}M_xTe$ near the Fermi level. (a) and (b) Reproduced with permission from ref 69. Copyright 2018, National Academy of Sciences, USA. (e) Reproduced with permission from ref 40. Copyright 2014, American Chemical Society.

DOI: 10.1021/acs.chemmater.8b02676
Chem. Mater. 2018, 30, 5799−5813

~1.61 at 823 K was obtained for $Ge_{0.86}Mn_{0.10}Sb_{0.04}Te$ via the combination of valence band convergence by MnTe alloying and carrier optimization by Sb in GeTe. Although Mn alloying in GeTe significantly reduces the valence band offset compared to Sb doping, the power factor decreases significantly in the Mn and Sb codoped sample due to high *p*-type carrier concentration. Thus, $Ge_{0.82}Mn_{0.10}Sb_{0.04}Te$ exhibits slightly lower zT of 1.61 compared to that of $Ge_{0.9}Sb_{0.1}Te$ (zT of 1.85). In addition, Liu et al.[69] have shown that codoping of Bi and Mn in GeTe leads to significantly high zT of ~1.5 at 773 K with average zT of ~1.1 from 300 to 773 K for the composition of $Ge_{0.81}Mn_{0.15}Bi_{0.04}Te$. This enhancement in zT was achieved due to the simultaneous process of suppression of Ge vacancies and *p*-type carrier density by Bi doping and modification of valence bands by Mn doping. Moreover, electronic structure calculations reveal that Mn doping in GeTe significantly increases the hole concentration and thereby pushes the Fermi level downward where multiple valence sub-bands are accessible, and those contribute for conduction.[69] From the band structure calculations, it is noteworthy to say that modification of DOS near the Fermi level along with the feasibility of accessing the multiple valence band upon Mn doping in GeTe is responsible for the observed high effective mass of 3.9 m_0 and the large Seebeck coefficient.

Symmetry-Breaking Strategy. The leading thermoelectric materials from the IV−VI family, especially PbTe and SnTe, have been known for rock-salt NaCl structure ($Fm\bar{3}m$) with double valence bands occurring at the L and Σ points in the Brillouin zone, which help them to exhibit high power factor of ~30 μW cm^{-1} K^{-2} and ~20 μW cm^{-1} K^{-2} for PbTe and SnTe, respectively.[74,75] Though, GeTe from the same family has not been explored well, it interestingly possesses a significantly high power factor of ~40 μW cm^{-1} K^{-2}.[76] The concrete reason behind the high power factor of GeTe was unclear until Li et al.[76] extensively performed the electronic structure calculation and realized that the high power factor is attributed to heavy Σ band contribution for conduction, whereas the light hole in the L band dominates the transport in both PbTe and SnTe. Moreover, electronic structure calculations have demonstrated that 8 half-valleys at the L band (4 equivalent L band) in cubic GeTe ($Fm\bar{3}m$) split into 6 half-valleys at the L point (3 equivalent L band) and 2 half-valleys at the Z point (1 equivalent Z band) in rhombohedral GeTe phase ($R3m$), while 12 full valleys of the Σ band in $Fm\bar{3}m$ split into 6 along Σ and other 6 along the η line (Figure 6a).[32,41] Notably, the valence band maximum at the L point in cubic GeTe shifts to heavy Σ band in rhombohedral GeTe during phase transition. As a result, heavier effective mass carriers of the Σ band dominate in transport properties in rhombohedral GeTe at room temperature, which, in fact, led to the unconventional enhancement in power factor in GeTe, unlike in PbTe and SnTe. Recently, Li et al.[41] have demonstrated slight symmetry reduction to rhombohedral GeTe from the cubic phase by Pb and Bi doping resulting in effective convergence of valence bands, which gave rise to the maximum zT of ~2.4 at 600 K and a device zT of 1.3 in the temperature range of 300−600 K (Figure 6b).[42] We believe this is an innovative strategy to enhance the thermoelectric performance in GeTe, which can be used for other thermoelectric materials.

Resonant States. Local distortion of density of states (DOS) by creating resonant states near the Fermi level can be an efficient strategy to enhance the Seebeck coefficient. This

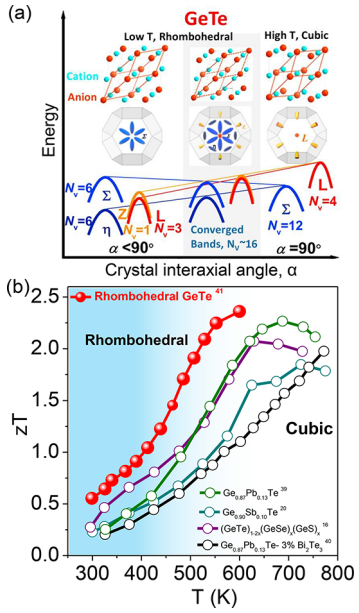

Figure 6. (a) Schematic energy diagram of the evolution of the electronic structure of GeTe from the cubic to the rhombohedral phase depending on the extent of symmetry reduction[41] and (b) temperature dependent thermoelectric figure of merit (zT) of rhombohedral GeTe ($Ge_{0.86}Pb_{0.10}Bi_{0.04}Te$) with state-of-the-art thermoelectric materials.[42] (a) and (b) Reproduced with permission from ref 41 and ref 42. Copyright 2018, Elsevier.

local enhancement in DOS within a small energy range can be realized when dopant energy level resonates with the valence or conduction band of the host semiconductor material. A fundamental relation between local change in DOS and *S* is given by Mott, which is given below,[77]

$$S = \frac{\pi^2 k_B^2}{3e} T \frac{d[\ln(\sigma(E))]}{dE} | E = E_F \quad (5)$$

where $\sigma(E)$ is energy-dependent electrical conductivity which is strongly dependent on DOS. Thus, distortion of DOS by introducing a resonant state in the parent materials is expected to increase the $\sigma(E)$ and thereby Seebeck coefficient. Resonant states induced unconventional DOS distortion has been realized in many of the IV−VI materials, such as Tl in PbTe,[6] Al in PbSe,[78] and In in SnTe.[7] Similarly, it has been shown that the DOS of GeTe near the Fermi level in the valence band can also be distorted by the group IIIA element of Ga and In at the Ge site in both rhombohedral and cubic GeTe (Figure 7a,b).[31] In particular, dopants of In and Ga induce two states, (i) the hyper-deep states at −5 to −6 eV well below the valence band and (ii) the deep defect states at around the Fermi level above valence band, which is more active and interestingly increases the energy-dependent electrical conductivity, $\sigma(E)$, by distorting the DOS at the Fermi level and supports enhancing the Seebeck value of GeTe as seen in Figure 7c. Further, these deep defect states (DDSs) are formed due to hybridization between resonant atoms (In/Ga) and host GeTe matrix. The fully filled valence band of GeTe becomes half-filled upon In doping, and every In atom doping at a Ge site generates one hole. Though both In and Ga create resonant levels in GeTe, the hybridization of In with its $5p^1$ rather than $5s^2$ in GeTe dominates and forms deep states well above the valence band, whereas energy levels from Ga get slightly deep into the valence band. So, In doping performs as

DOI: 10.1021/acs.chemmater.8b02676
Chem. Mater. 2018, 30, 5799−5813

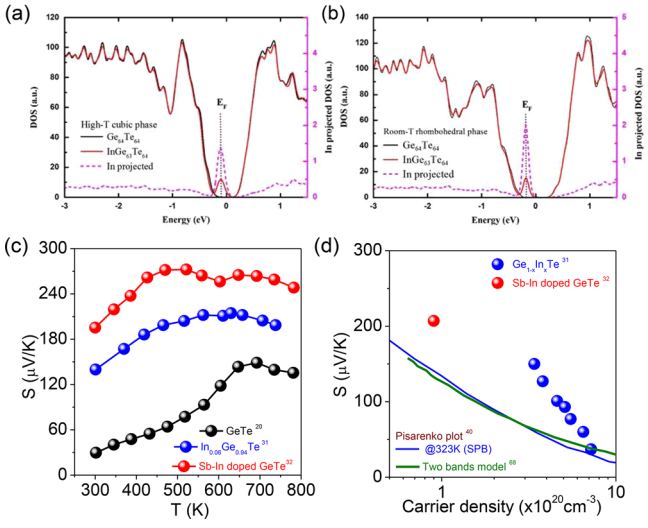

Figure 7. Density of states (DOS) of (a) high temperature cubic phase $Ge_{64}Te_{64}$ and $Ge_{63}InTe_{64}$ and (b) room temperature rhombohedral phase $Ge_{64}Te_{64}$ and $Ge_{63}InTe_{64}$.[31] (c) Temperature dependent Seebeck coefficient (S) of In doped and In and Sb codoped GeTe. (d) Seebeck coefficient vs carrier concentration plot for In and Sb doped GeTe samples at 323 K. (a) and (b) are reproduced with permission from ref 31. Copyright 2017 Nature Publishing Group (http://creativecommons.org/licenses/by/4.0/).

an efficient resonant dopant in GeTe in order to distort DOS near the Fermi level. Due to the indium induced DOS distortion, the sample of 5 mol % of In-doped GeTe has shown the Seebeck value of 137 μV/K at 300 K which is significantly high and strongly deviated from the Pisarenko line plotted from experimental S vs n as shown in Figure 7d.[31] Moreover, a maximum power factor of 42 μW cm^{-1} K^{-2} and the highest zT of ∼1.3 was achieved for the composition of $Ge_{0.98}In_{0.02}Te$. Recently, Hong et al.[32] have achieved the significantly high zT of ∼2.3 at 680 K and average zT of ∼1.6 in Sb and In codoped GeTe, where doping of Sb, In, and Sb−In has been associated with reduction in carrier density, formation of resonant states by distortion of DOS near the Fermi level, and increase of the valley degeneracy via room temperature phase transition from low symmetry $R3m$ to high symmetry $Fm\bar{3}m$ structure, respectively. Interestingly, the electronic structure calculation with spin−orbital coupling has demonstrated that low symmetry ($R3m$) GeTe has 6 full valleys at the heavy Σ point, whereas high symmetry cubic ($Fm\bar{3}m$) GeTe consists of 12 full valleys at the Σ point with 8 half-valleys at the L point, which is the reason behind high thermoelectric performance in Sb and In codoped GeTe.[32] In this context, the S value of $Ge_{0.88}Sb_{0.12}Te$ was to be ∼155 μV/K at 300 K (Figure 7d), while S of $Ge_{0.888}Sb_{0.12}In_{0.02}Te$ has increased to ∼195 μV/K due to a large change in the DOS near the Fermi level by In states along with p-type carrier optimization and band convergence by Sb doping.[20,32] The observed S values of $Ge_{1-x-y}Sb_xIn_yTe$ were also deviated from the Pisarenko line at 323 K (Figure 7d), which is an evidence for the contribution from the second valence bands and DOS modification due to the resonance level.

REDUCTION OF THE LATTICE THERMAL CONDUCTIVITY

Heat in crystalline solids is generally transported by charge carriers, phonons, magnons, and excitation, but in thermoelectric degenerate semiconductors, heat is mainly transported by charge carriers and phonons.[3,79] As the electronic component of the thermal conductivity is strongly related to electrical conductivity through the Wiedemann−Franz law ($\kappa_{el} = L\sigma T$), it is not beneficial to decrease the κ_{el} owing to linear dependence of the power factor to electrical conductivity.[2] Lattice thermal conductivity (κ_{lat}) is the only materials property that can be manipulated independently to enhance zT of the TE materials. Years of research to decrease the lattice thermal conductivity has come up with different promising strategies. Introduction of various types of crystal defects, viz., point defects (0D), dislocations (1D), interfaces (2D), and formation of grain boundaries, are the two traditional strategies to reduce lattice thermal conductivity by accelerating the scattering rates of phonon waves.[79] The concept of endotaxial nanostructuring is proven to be effective to reduce κ_{lat} by utilizing the phonon-interface scattering mechanism, without severely affecting the charge carrier mobility. Unfortunately, most of the phonon scattering mechanisms are prevailing toward a certain range of phonon frequencies (i.e., while point defect scattering targets high frequency phonons; 2D interfacial scattering, grain boundaries, or fine nanoprecipitates dominantly scatter low frequency phonons),[79] thus the entire scale hierarchical phonon scattering mechanism is desired to achieve κ_{min} in a particular thermoelectric material.[13]

GeTe exhibits superior electronic properties as well high power factor owing to unique electronic structure as discussed in the previous section, whereas GeTe possesses quite a high κ_{lat} of ∼2.7 W/(m K) despite having a very low theoretical minimum limit of κ_{lat} (κ_{min} ∼ 0.3 W/(m K)), which is indeed restricting high thermoelectric performance of GeTe.[22] Recently, GeTe based materials stand out to be one of the best-performed thermoelectric materials due to reasonably low κ_{lat}. Here below, all the major recent tactics employed recently to reduce the κ_{lat} of GeTe are discussed (Figure 8).

Solid Solution Alloying. Alloying or doping is effective to decrease the κ_{lat} of materials by introducing atomic disorder

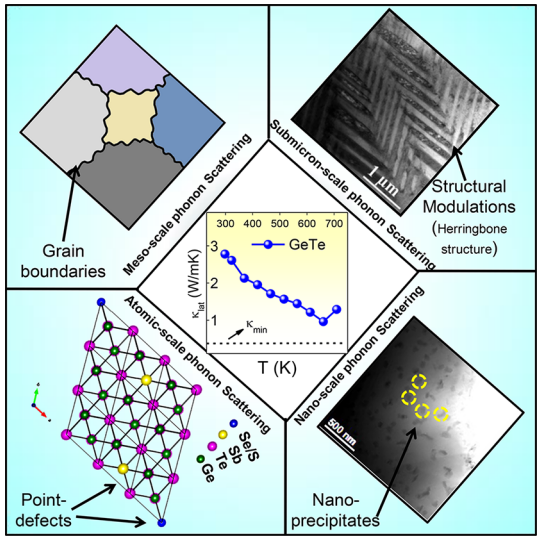

Figure 8. Illustration showing the different phonon scattering mechanisms for reducing lattice thermal conductivity (κ_{lat}) of GeTe. Reproduced with permission from ref 16, copyright 2017, American Chemical Society; ref 20, copyright 2015, American Chemical Society; and ref 35, copyright 2017, John Wiley and Sons.

DOI: 10.1021/acs.chemmater.8b02676
Chem. Mater. 2018, 30, 5799−5813

(either substitutionally or interstitially) in the crystal lattice, which is generally considered as point defects. Alloying or doping leads to the mass contrast between foreign atoms and regular lattice sites, which indeed enhances the phonon scattering rate. Frequency dependence of the point defect phonon scattering relaxation time (τ_{PD}) is given by the following equation:[80]

$$\tau_{PD}^{-1} = \frac{V\omega^4}{4\pi v_s^3}\left(\sum_i f_i\left(1 - \frac{m_i}{\bar{m}}\right)^2 + \sum_i f_i\left(1 - \frac{r_i}{\bar{r}}\right)^2\right) = \frac{V\omega^4}{4\pi v_s^3}\Gamma = A\omega^4 \quad (6)$$

where V is the average volume per atom, ω is the phonon frequency, and f_i is the fraction of atoms with mass m_i and radius r_i on a crystallographic site with average mass $\bar{m}$ and radius $\bar{r}$. Γ is the disorder scattering parameter which equates to $\Gamma = \Gamma_{MF}$ (mass fluctuation term) + Γ_{SF} (strain field term). Thus, the higher the mass and size mismatched between the host and the foreign atom, the higher the phonon scattering.

Alloying/doping of the parent (host) compound with another foreign element can be driven by enthalpy, entropy, or both depending upon the miscibility between the host and the foreign compounds. When host and foreign compounds are completely miscible for a certain percentage of foreign compounds (x%), alloying is mainly driven by the enthalpy of the system, which is a major case for the alloying between two binary systems. Figure 9 shows a comparison of lattice thermal conductivity (κ_{lat}) of different GeTe-based samples at room temperature, where reduction in κ_{lat} of samples is mainly ascribed to point defect phonon scattering. Alloying of GeTe with Sb causes a significant reduction in κ_{lat} which is due to effective phonon scattering from point defects, domain structures, and twin, inversion, and grain boundaries, e.g., κ_{lat} of GeTe decreases from 2.7 W/(m K) to ~1.4 W/(m K) in the $Ge_{0.90}Sb_{0.10}Te$ sample.[20] Further lowered ~κ_{lat} in $Ge_{1-x}Sb_xTe$ samples can be achieved by introducing additional point defects by Se alloying (κ_{lat} ~ 0.8 W/(m K) in $Ge_{0.85}Sb_{0.15}Te_{0.88}Se_{0.12}$).[68] Alloying of MnTe with GeTe causes colossal reduction in κ_{lat} in the range of ~0.25−0.5 W/(m K) at 800 K, approaching the κ_{min} of GeTe.[73,81] Mn in $Ge_{1-x}Mn_xTe$ introduces enhanced mass fluctuations as well as creates strain field (because of radius mismatch of Mn and Ge) which serves as phonon scattering centers. Moreover, MnTe alloying with GeTe softens the chemical bonds, thereby decreasing phonon group velocity, which further reduces the κ_{lat} (eq 1). Co-doping is also an effective way to reduce κ_{lat} by introducing increased point defects arising from both the dopants. Considerably low κ_{lat} of ~0.7 W/(m K) is realized in Pb and Bi codoped GeTe samples at room temperature because of the synergistic effect of mass and size fluctuations resulting from both Pb and Bi doping.[41] Sb and In codoping in GeTe resulted in significantly reduced κ_{lat} (~0.72 W/(m K) in $Ge_{0.89}Sb_{0.1}In_{0.01}Te$ at 300 K) which is mainly ascribed to extrinsically strengthened phonon scattering due to grain boundaries, point defects, and stacking faults within the cubic phase of GeTe.[32] Recently, alloying of PbSe with GeTe resulted in ultralow κ_{lat} of ~0.5 W/(m K) at 300 K, which is driven by enhanced point defect scattering benefiting from both cation and anion disorders.[82]

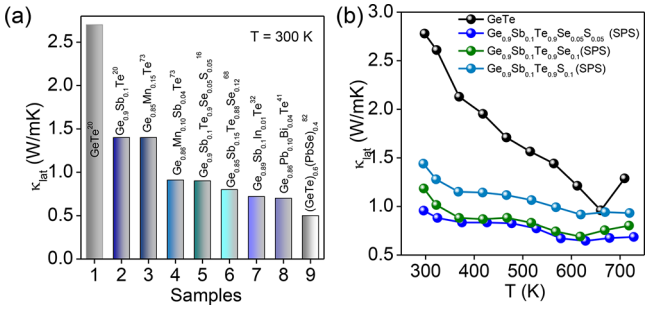

Figure 9. Comparison of lattice thermal conductivity (κ_{lat}) of GeTe-based materials at room temperature. Reductions of κ_{lat} of all the samples are ascribed to the phonon scattering due to point defects. (b) Temperature variation of κ_{lat} of GeTe, $Ge_{0.9}Sb_{0.1}Te_{0.9}Se_{0.05}S_{0.05}$, $Ge_{0.9}Sb_{0.1}Te_{0.9}Se_{0.1}$ and $Ge_{0.9}Sb_{0.1}Te_{0.9}S_{0.1}$, representing a pseudoternary system, is superior to achieve low κ_{lat} compared to that of the binary system.[16]

Entropy engineering is an effective approach to reduce the κ_{lat} of a system via formation of extensive point defects which can inhibit the propagation of heat-carrying phonons. Ternary systems such as PbTe−PbSe−PbS or GeTe−GeSe−GeS are expected to have higher degree of disorder, i.e., higher entropy compared to that in binary systems such as PbTe−PbSe or GeTe−GeSe.[16,83] In spite of poor miscibility between GeTe and GeS, ternary $(GeTe)_{1-2x}(GeSe)_x(GeS)_x$ forms entropy driven extended solid solution up to a certain percentage of GeS (10 mol %). When GeS concentration exceeded 10 mol %, phase separation of GeS rich 5−30 μm sized GeS precipitates occurred into the $GeTe_{1-x}Se_x$ matrix. These bigger precipitates do not effectively participate to scatter the heat carrying phonons in GeTe as the mean free path of the heat carrying phonon ranges 1−100 nm. Rather, such an entropy driven system existed with full of point defects and disorder, which have been verified by fitting the experimental κ_{lat} data by Callaway's model. A low κ_{lat} of ~0.91 W/(m K) was achieved in $(GeTe)_{0.9}(GeSe)_{0.05}(GeS)_{0.05}$ at 710 K. Sb alloying and spark plasma sintering (SPS) of the $(GeTe)_{0.9}(GeSe)_{0.05}(GeS)_{0.05}$ sample further suppressed the κ_{lat} to as low as ~0.7 W/(m K) at 728 K because of excess phonon scattering due to entropy driven solid solution point defects and grain boundaries.[16] Figure 9b exhibits the comparison of κ_{lat} among of GeTe, $Ge_{0.9}Sb_{0.1}Te_{0.9}Se_{0.05}S_{0.05}$, $Ge_{0.9}Sb_{0.1}Te_{0.9}Se_{0.1}$ and $Ge_{0.9}Sb_{0.1}Te_{0.9}S_{0.1}$. $Ge_{0.9}Sb_{0.1}Te_{0.9}Se_{0.05}S_{0.05}$ exhibits the lowest κ_{lat} among them showing the effectiveness of the entropy driven point defects involving a broad set of multiple types of mass fluctuations both in cation and in anion sites of GeTe such as Ge/Sb, Te/Se, Te/S, and Se/S.

Nanostructuring. Nanostructuring in the form of nanoprecipitates is one of the most anticipated strategies in thermoelectrics for reducing lattice thermal conductivity by scattering phonons with mid to long wavelengths. Interestingly, for IV−VI metal tellurides, namely, PbTe, SnTe, and GeTe, more than 90% of κ_{lat} is dominated by the phonons having mean free paths in the range of 1−100 nm.[32,60] Thus, nanostructuring is believed to be an effective pathway to reduce the κ_{lat} of the GeTe (Figure 10). Pseudobinary $(GeTe)_x(AgSbTe_2)_{100-x}$ (TAGS-x) alloys are best recognized for their low κ_{lat} (~0.8 W/(m K) in TAGS-85 and 1 W/(m K) in TAGS-80 at room temperature), which is mainly attributed to the presence of second phases (Ag_8GeTe_6, Ag_6GeTe_5, and $Ag_2Ge_{85}SbTe_{10}$ in TAGS-85 and Ag_3GeTe_2 in TAGS-80) as

DOI: 10.1021/acs.chemmater.8b02676
Chem. Mater. 2018, 30, 5799−5813

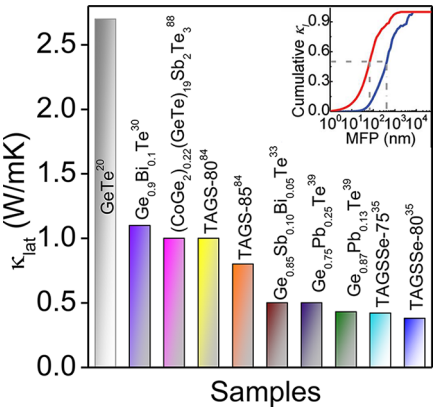

Figure 10. Comparison of lattice thermal conductivity (κ_{lat}) of different GeTe-based nanostructured samples at room temperature (300 K). Inset shows the normalized cumulative κ_l with phonon mean free paths (MFPs) of rhombohedral GeTe (R-GeTe, blue line) and cubic GeTe (C-GeTe, red line) between 1 nm and 10 μm at 300 K.[32] Inset figure, reproduced with permission from ref 32. Copyright 2018, John Wiley and Sons.

nanostructures (Figure 11a,b) and nano-/microstructure modulations (twin boundaries, inversion boundaries, herring-

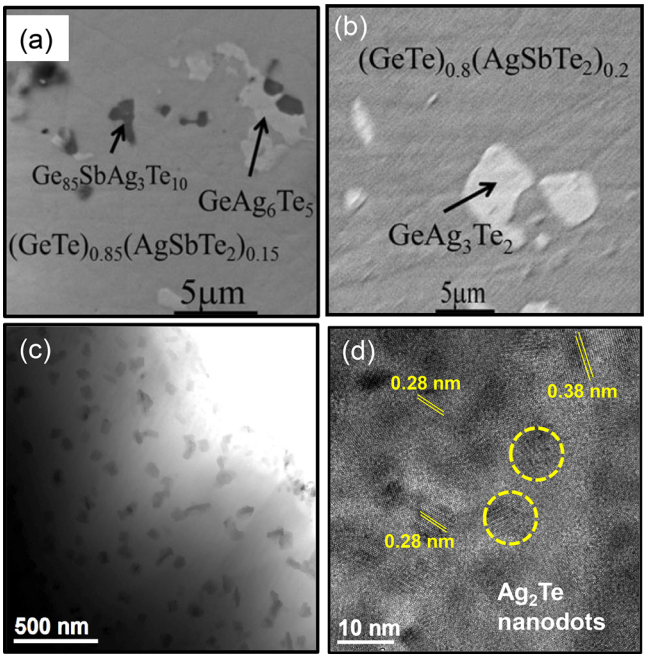

Figure 11. (a) and (b) Nanoprecipitates in TAGS-85[84] and TAGS-80,[84] respectively. (c) Low magnification TEM image of TAGSSe-75[35] showing the homogeneous distribution of Ag_5Te_3 nanoprecipitates in the GeTe-rich matrix. (d) High-Resolution TEM micrograph of TAGSSe-75 confirms the presence of Ag_2Te nanodots. (a) and (b) Reproduced with permission from ref 84. Copyright 2012, TMS. (c) and (d) Reproduced with permission from ref 35. Copyright 2017, John Wiley and Sons.

bone structures, antiphase domain, etc.) in the GeTe rich matrix.[84−86] Another series of pseudobinary compound $(GeTe)_x(AgSbSe_2)_{100-x}$ (TAGSSe-x) have been recently explored to exhibit ultralow κ_{lat} throughout the measured temperature (300−700 K), viz., TAGSSe-80 exhibits a κ_{lat} value of ∼0.4 W/(m K) in the 300−700 K range, which is indeed close to the κ_{min} of GeTe.[35] Transmission electron microscopy (TEM) of TAGSSe-80 and TAGSSe-75 reveals homogeneous distribution of Ag_2Te nanodots (2−6 nm) and Ag_5Te_3 nanoprecipitates (20−80 nm) embedded in the GeTe-rich matrix along with grain boundaries (Figure 11c,d). This hierarchical nano-/meso-structuring in the GeTe matrix resulted in significant scattering of the phonon with different wavelengths to gives rise to ultralow κ_{lat} in TAGSSe-x (x = 80, 75).

Ge rich $Ge_{1-x}Pb_xTe$ is a unique system to study the correlation between nano-/microstructures and κ_{lat} (Figure 12a).[38−40,87] When the concentration of Pb in $Ge_{1-x}Pb_xTe$

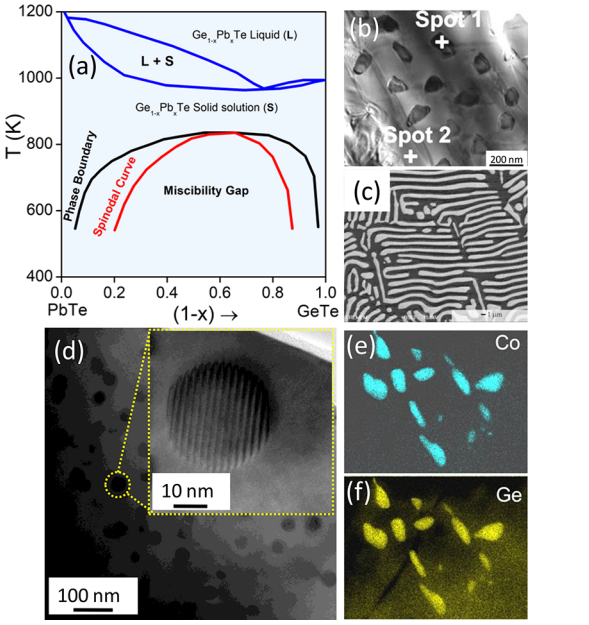

Figure 12. (a) Quasi-binary phase diagram of the GeTe-PbTe system depicting miscibility gap of GeTe and PbTe. (b) TEM micrograph of $Ge_{0.87}Pb_{0.13}Te$ showing presence of spherical precipitates of PbTe (spot 1) in the GeTe rich matrix (spot 2).[40] (c) SEM-BSE image $Ge_{0.64}Pb_{0.36}Te$ showing lamellar precipitates of PbTe (darker region) in GeTe-rich matrix (lighter region) formed by spinodal decomposition mechanism.[87] (d) Low magnification TEM image of $Ge_{0.85}Sb_{0.1}Bi_{0.05}Te$ showing the homogeneous distribution of Bi rich nanoprecipitates in the GeTe-rich matrix.[33] Inset shows a zoomed version of the nanoprecipitates. (e) and (f) STEM-EDX element mapping of $(CoGe_2)_{0.2}(GeTe)_{17}Sb_2Te_3$ sample confirming the presence of $CoGe_2$ nanoprecipitates.[88] (b) Reproduced with permission from ref 40. Copyright 2014, American Chemical Society. (c) Reproduced with permission from ref 87. Copyright 2010, American Chemical Society. (d) Reproduced with permission from ref 33. Copyright 2017, American Chemical Society. (e) and (f) Reproduced with permission from ref 88. Copyright 2015, American Chemical Society.

exceeds x = 5 mol %, it undergoes phase separation into PbTe rich regions in the GeTe matrix. When x is 0.20 > x > 0.05 (in between the phase boundary and the spinodal curve), phase separation is mainly dominated by the nucleation and growth mechanism giving spherical nanoprecipitates (50−100 nm) of PbTe in GeTe-rich matrix (Figure 12b).[38,40] When x falls in the miscibility gap of the GeTe−PbTe system (under the spinodal curve), spinodal decomposition takes the lead which results in phase separation into lamellar PbTe rich precipitates in GeTe matrix (Figure 12c).[39,87] In both the cases, κ_{lat} of the $Ge_{1-x}Pb_xTe$ system decreases drastically compared to that of

DOI: 10.1021/acs.chemmater.8b02676
Chem. Mater. 2018, 30, 5799−5813

the pristine GeTe sample, although nucleation is favored over spinodal decomposition as finer nanostructures are desired to reduce κ_{lat}. κ_{lat} values of $Ge_{0.87}Pb_{0.13}Te$ and $Ge_{0.75}Pb_{0.25}Te$ are ~0.4 W/(m K) and ~0.5 W/(m K), respectively, at 323 K.[38,39] Excess Bi addition (10 mol %) in GeTe forms Bi rich nanoprecipitates in the GeTe matrix, which reduces the κ_{lat} of the sample, e.g., $Ge_{0.9}Bi_{0.10}Te$ exhibits κ_{lat} of ~1.1 W/(m K) at 300 K.[30] Moreover, Bi and Sb codoped GeTe samples exhibit significantly low κ_{lat} (~0.5 W/(m K)) because of synergistic phonon scattering by the Bi rich nanoprecipitates (Figure 12d) and atomic-scale point defects created by substitution of Sb in GeTe.[33] $(CoGe_2)_{0.22}(GeTe)_{19}Sb_2Te_3$ shows considerably low κ_{lat} ~ 1 W/(m K) at 323 K whereas control sample $(GeTe)_{19}Sb_2Te_3$ (GST) exhibits κ_{lat} of ~1.6 W/(m K) at 323 K. This difference in κ_{lat} between $(CoGe_2)_{0.22}(GeTe)_{19}Sb_2Te_3$ and $(GeTe)_{19}Sb_2Te_3$ samples is mainly attributed to homogeneous distributions of cobalt−germanide nanoprecipitates in the GST matrix (Figure 12e,f) which lead to enhanced phonon scattering in $(CoGe_2)_{0.22}(GeTe)_{19}Sb_2Te_3$.[88]

LAYERED GERMANIUM CHALCOGENIDES

Layered metal chalcogenides provide intriguing electronic properties owing to their two-dimensional crystal structure and offer diverse opportunities for thermoelectrics. Recently, the discovery of an unprecedentedly high thermoelectric figure of merit (zT) of ~2.6 in SnSe has created a sensation in thermoelectric research.[5,43] The observed zT arises from a favorable combination of large Seebeck coefficient resulting from multiple valence bands near the Fermi level and ultralow κ_{lat} due to strong anharmonicity. The discovery of SnSe has drawn attention to the study of other lead-free layered two-dimensional chalcogenides from the IV−VI family.

At ambient condition, GeSe has a layered crystal structure (space group, *Pnma*) similar to that of SnSe. Based on temperature and pressure, GeSe crystallizes in three dissimilar crystal structures, namely, orthorhombic (space group, *Pnma*), rhombohedral (space group, *R*3*m*), and cubic (space group, $Fm\bar{3}m$) (Figure 13).[23] In this perspective, we will discuss in detail how this structural transition affects the thermoelectric properties of GeSe.

Recently, Hao et al. predicted high thermoelectric performance in GeSe because of its favorable electronic structure (multivalence band) and extremely low κ_{lat} by using first principles DFT calculation (Figure 14).[25] The experimentally measured electronic band gap for orthorhombic GeSe is 1.1 eV

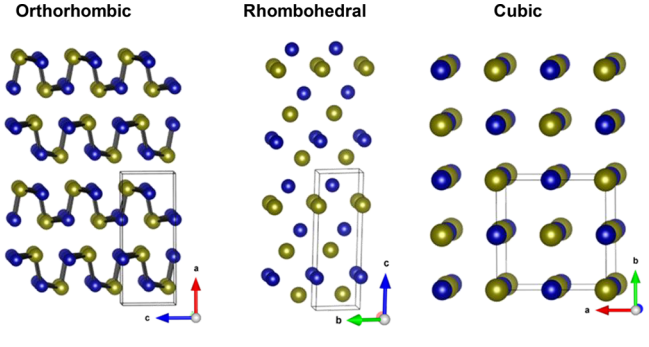

Figure 13. Crystal structure of (a) orthorhombic (*Pnma*), (b) rhombohedral (*R*3*m*), and (c) cubic ($Fm\bar{3}m$) GeSe (green and blue atoms are Ge and Se, respectively).

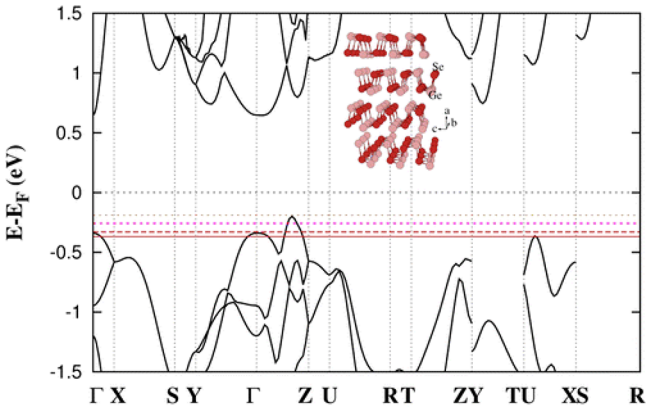

Figure 14. Electronic structure of orthorhombic GeSe at different dopant concentrations (5×10^{17}, 5×10^{19}, 2×10^{20}, and 4×10^{20}). Reproduced with permission from ref 25. Copyright 2016, American Chemical Society.

which is much higher compared to that of GeTe.[22,23] For the *Pmna* phase of GeSe, the first and second valence band maximum is positioned in the Γ−Z direction and at the Γ point, respectively (Figure 14). The energy difference of the first two valence bands is ~0.13 eV which is smaller compared to that of PbTe (~0.15 eV). The third valence band exists along the U−X direction within a small energy difference. The energy separation of the first and third maxima (~0.16 eV) is comparable to the spacing between the first and the second valence band edges of PbTe, where heavy hole contribution can be significant with a carrier density of 5×10^{19} cm^{-3} (Figure 14).[25] This indicates a significant contribution from those entire valence bands when the carrier concentration reaches ~5×10^{19} cm^{-3}. The presence of multiple valence bands within a small energy region can be illustrated as the Fermi surface with multiple pockets. Due to anisotropic lattice dynamics, the band effective masses of each valence band maximum are different. The observed high Seebeck coefficient in GeSe (~470 μV/K at 300 K)[24] is mainly arising from the multiband effect similar to that of orthorhombic SnSe (S ~ 480 μV/K at 300 K).[89,90] Theoretically it is predicted that the thermal conductivity of GeSe should be lower than that of SnSe because of the high Gruneisen parameters of GeSe (γ = 2.6) compared to SnSe (γ = 2.3), mainly ascribed to the intriguing crystal structure (distorted GeSe polyhedral) of GeSe.[25] However, experimentally SnSe exhibits lower κ_{lat} (~1 W/(m K) at 300 K) compared to GeSe (κ_{lat} ~ 1.8 W/(m K) at 300 K).[24]

High Seebeck coefficient of the multiband system and low thermal conductivity made GeSe an ideal material for thermoelectric investigations. The experimentally observed zT for orthorhombic GeSe is only 0.06 at 720 K which is far below the theoretically predicted value (~2.5 at 800 K).[24] The main reason for its poor performance is its low electrical conductivity due to extremely low carrier concentration (10^{17} cm^{-3}). This leaves the primary motivation for the researchers to focus on improving the carrier concentration of GeSe. *p*-type dopants such as Ag, Cu, and Na and n-type dopants like Sb, Bi, La, I, and As have been attempted to improve the carrier concentration of GeSe, but the achieved zT values are far from the theoretical value.[24]

At 930 K, GeSe undergoes a structural transition from orthorhombic to high symmetry face-centered cubic (FCC) structure. It is not possible to get the high-temperature cubic

DOI: 10.1021/acs.chemmater.8b02676
Chem. Mater. 2018, 30, 5799−5813

phase of GeSe at ambient conditions due to the existence of various imaginary vibration modes in its phonon dispersion which can be stabilized by applying external pressure as predicted by first principles theoretical calculation (Figure 15).[91] Recently, Huang et al. have stabilized the *p*-type

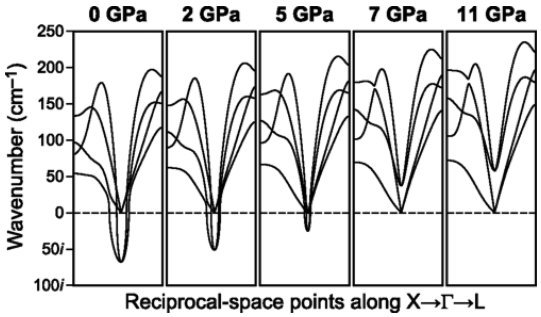

Figure 15. Variation of phonon dispersion of cubic GeSe with simulated external pressure (0−11 GPa). Reproduced with permission from ref 91. Copyright 2014, American Physical Society.

rhombohedral GeSe phase (space group *R*3*m*; $a = b = 3.958$ Å and $c = 10.081$ Å) by alloying it with $AgSbSe_2$, which showed a promising thermoelectric figure of merit of 0.86 at 710 K.[23] The high thermoelectric performance is mainly coming from the high carrier concentration ($\sim 10^{20}$ cm^{-3}) resulting from the multivalley Fermi surface of the rhombohedral phase. The measured κ_{lat} for the $AgSbSe_2$ alloyed GeSe sample (0.9 W m^{-1} K^{-1}) is still higher than its theoretical κ_{min} value (0.4 W m^{-1} K^{-1}). Moreover, the $AgSbSe_2$ alloyed GeSe sample reduces the transition temperature to cubic GeSe from 930 to 523 K. Calculated electronic structure of rhombohedral GeSe is similar to that of rhombohedral GeTe. Combination of more conduction pockets and high effective mass improves the zT of rhombohedral GeSe compared to orthorhombic GeSe. Moreover, $AgSbTe_2$ alloying further enhances the thermoelectric figure of merit from 0.06 to ∼1 at 754 K by converging light and heavy valence bands.[92] This indicates that rhombohedral GeSe could be a promising thermoelectric material which is made of more earth-abundant elements with less toxicity.

Recently, Fabian O. von Rohr et al. have synthesized and calculated the electronic structure of the new *β*-GeSe.[93] The *β*-GeSe exhibits a boat conformation for its Ge−Se six-membered ring. Formation of *β*-GeSe was only attainable at high pressure and temperature, but it is stable even at ambient conditions after the release of temperature and pressure.[93] Electronic structure calculation confirms the semiconducting nature of *β*-GeSe, and favorable band gap (bulk: 0.5 eV) makes it a promising candidate for practical applications.[93]

GeS, 2D layered germanium monochalcogenide, crystallizes in orthorhombic structure (space group, *Pnma*) at ambient condition similar to its analogue, GeSe. The theoretically predicted band gap for GeS is ∼1.22 eV which is higher compared to that of GeSe (0.85 eV) and SnSe (0.61 eV).[25] Unlike SnSe and GeSe, GeS accesses the light hole valence band upon increasing hole carrier concentration by doping. Thus, the multiband effect with high carrier concentration is not an effective approach to increase the Seebeck coefficient of GeS. At the same time, κ_{lat} of GeS is higher compared to that of SnSe and GeSe. As a result of all the above facts, pristine GeS is not a good candidate for thermoelectric application until proper optimization of the thermoelectric parameters happens.[25]

Apart from the binary layered germanium chalcogenides (GeSe/S), various layered intergrowth ternary Ge chalcogenide based compounds exist which belong to the homologous family of $Ge_zM_{2n}X_{z+3n}$ (M = Sb, Bi; X = Te, Se), where *z* and *n* represent the stoichiometry of GeX and M_2X_3, respectively. $GeBi_2Te_4$ and $GeSb_2Te_4$ from this homologous family have topologically protected surface state which is recently verified experimentally and theoretically.[94] $GeBi_2Te_4$ is one of the peritectic compounds in the pseudobinary phase diagram of $GeTe-Bi_2Te_3$ and crystallizes in rhombohedral structure (space group $R\bar{3}m$) with 21 layers in each unit cell. Schroder et al. have stabilized the metastable $GeBi_2Te_4$ at 12 GPa.[95] Interestingly, $GeBi_2Te_4$ exhibits ultralow lattice thermal conductivity ($\kappa_{lat} \sim 0.5$ W/(m K) at 300 K)[95] because of the high molecular weight of Bi and Te and anisotropic layered structure. This class of compounds has high technological importance owing to their phase change behavior (crystalline to amorphous) which can be used in the rewritable storage device. Importantly, GST ($GeTe-Sb_2Te_3$) based materials have wide applications in rewritable storage device.

CONCLUSIONS AND OUTLOOK

Research on GeTe has attracted significant attention from the material facet to the device stage owing to their superior thermal and mechanical stability. In this perspective, we have discussed the state-of-art strategies such as carrier concentration optimization, electronic structure engineering via resonant level formation, and valence band convergence and crystal defect engineering and nanostructuring approach to optimize the thermoelectric properties of germanium chalcogenide based materials. These well-proven strategies enhance one thermoelectric parameter explicitly with reverse consequences on other thermoelectric parameters restricting the significant improvement of overall performance because of the interconnected nature of thermoelectric parameters. Nevertheless, these give us an indication of the huge scope of research to improve the TE performance by decoupling interdependent parameters. Synergistic improvement on computational methods and advanced synthesis techniques may help researchers to manipulate each and every parameter further and decouple them to reach a thermoelectric figure of merit of c.a. > 3 in germanium chalcogenide based materials. The main constraint for the improvement of thermoelectric performance of GeTe comes from its intrinsic high *p*-type carrier concentration which needs to be solved. Recently, we have shown that Sb is an effective dopant to solve this issue partly. Interestingly, GeTe is the only material in the IV−VI family which crystallizes in the rhombohedral structure at an ambient condition which has polar Ge and Te bonds, resulting in ferroelectricity in the structure which has a strong influence on the transport properties. Near the ferroelectric phase transition, the thermal conductivity decreases to its minimum value owing to strong optic-acoustic phonon coupling and makes enormous room for further studies on the phase transition of GeTe to achieve the minimum thermal conductivity near room temperature.

Although remarkable efforts have been made to improve TE performance of materials in the last few decades, the progress of research on the high-performance TE device is still very slow. In spite of tremendous improvement of thermoelectric performances of *p*-type GeTe based materials, hardly any efforts have been made to construct a device or module for the real-life application.[96] Moreover, the high mechanical strength

DOI: 10.1021/acs.chemmater.8b02676
Chem. Mater. 2018, 30, 5799−5813

(Vickers microhardness of ∼209 H_V) and thermal stability of GeTe-based thermoelectric materials[16,20,22,35] compared to other IV−VI chalcogenides such as PbTe/SnTe makes it a suitable and potential candidate for device applications. Therefore, significant attention should be given to GeTe based device fabrication.

Compatibility is another issue for fabrication of any thermoelectric module or device. Better compatibility of any thermoelectric device or module demands both a *p*- and an *n*-type leg made of the same materials. Though there are significant advances of the thermoelectric performance of *p*-type Ge-based chalcogenides, hardly any *n*-type Ge-based chalcogenide is known hitherto. High hole carrier concentration in GeTe makes it difficult to change the carrier type from *p*-type to *n*-type. So, new methods/strategies are required to develop high-performance *n*-type GeTe based materials.

Although high thermoelectric performance is predicted in orthorhombic GeSe because of its favorable electronic structure (multivalence band) and extremely low thermal conductivity by using first principles DFT calculation, the experimental realization is far below from the expected zT value due to low carrier concentration which hints about the enormous research opportunities to further improve the thermoelectric performance of GeSe.

Besides the above-mentioned physical phenomena, new concepts or ideas to enhance the performance are always required to understand the transport properties via chemical intuition, where a material chemist can play a major role to fulfill the above-mentioned demands. Exploiting new materials with unique structural attributes is a reliable approach for achieving high thermoelectric performance. Fundamental properties of a material such as band gap, band degeneracy, effective mass, bond strength, bonding nature, and electronegativity should also be used to understand the thermoelectric transport properties. Recent advancement in high-throughput calculations can help to identify new and efficient materials for practical applications.

In summary, germanium chalcogenide based materials exhibit significant thermoelectric performance and can be an alternative solution for lead chalcogenides for mid-temperature power generation. Here, we have discussed the progress and future challenges to improve the thermoelectric performance of germanium chalcogenides by focusing on their crystal and electronic structure and lattice dynamics. Although state-of-the-art strategies have improved the thermoelectric performance of germanium chalcogenide-based material, still much work has to be done to enhance the performance of both materials and devices. Thus, we believe that this perspective will enhance the communication between chemists, physicists, and material and device engineers to make rapid progress in the field of thermoelectric research and provide a promising future for mass-market applications.

AUTHOR INFORMATION

Corresponding Author

*(K.B.) E-mail: kanishka@jncasr.ac.in.

ORCID

Kanishka Biswas: 0000-0001-9119-2455

Notes

The authors declare no competing financial interest.

Biographies

Subhajit Roychowdhury received his B.Sc. (2012) degree from University of Burdwan and M.Sc. (2014) degree in Chemistry from Indian Institute of Technology (IIT), Kharagpur, West Bengal, India. He is currently pursuing his Ph.D. under Prof. Kanishka Biswas at New Chemistry Unit, Jawaharlal Nehru Centre for Advanced Scientific Research (JNCASR), Bangalore, India. His research topics focus on topological insulators and thermoelectric properties of heavy metal chalcogenides.

Manisha Samanta obtained her B.Sc. (2013) degree from University of Burdwan and M.Sc. (2015) degree in Chemical Sciences from Indian Institute of Technology (IIT), Chennai, India. She is currently pursuing her Ph.D. under the guidance of Prof. Kanishka Biswas at New Chemistry Unit, Jawaharlal Nehru Centre for Advanced Scientific Research (JNCASR), Bangalore, India. Her research areas focus on investigations of thermoelectric properties of germanium chalcogenides and 2D layered materials.

Suresh Perumal received his Ph.D. (2013) at Materials Research Centre in Indian Institute of Science, India, under the supervision of Prof. A. M. Umarji. He was a Postdoctoral Fellow in Prof. Kanishka Biswas's lab in New Chemistry Unit, JNCASR, Bangalore, India, and also with Prof. Franck Gascoin at Laboratoire CRISMAT-ENSICAEN, University of Caen, France. He has recently joined SRM Institute of Science and Technology, Chennai, India, as an Assistant Professor. His research expertise is in synthesis, materials processing and physical properties of intermetallics, and silicides and chalcogenides for thermoelectric devices.

Kanishka Biswas obtained M.S. and Ph.D. degrees from the Solid State Structural Chemistry Unit, Indian Institute of Science, Bangalore, India (2009), under the supervision of Prof. C. N. R. Rao and did postdoctoral research with Prof. Mercouri G. Kanatzidis at the Department of Chemistry, Northwestern University, Evanston, IL, U.S.A. (2009−2012). He started his independent career in 2012, and currently, he is an Associate Professor in the New Chemistry Unit, Jawaharlal Nehru Centre for Advanced Scientific Research (JNCASR), Bangalore. He is pursuing research in the solid-state inorganic chemistry of metal chalcogenides and halides, thermoelectrics, topological materials, 2D materials, and water purification (http://www.jncasr.ac.in/kanishka/).

ACKNOWLEDGMENTS

The thermoelectric program in our group based on GeTe is mainly supported by DST (DST/TMD/MES/2k17/24). S.R. and M.S. thank CSIR and UGC, respectively, for fellowships. We express regret to the authors whose work we could not cite in this article due to space constraints.

REFERENCES

(1) Tan, G.; Zhao, L.-D.; Kanatzidis, M. G. Rationally designing high-performance bulk thermoelectric materials. *Chem. Rev.* **2016**, *116*, 12123−12149.

(2) Sootsman, J. R.; Chung, D. Y.; Kanatzidis, M. G. New and old concepts in thermoelectric materials. *Angew. Chem., Int. Ed.* **2009**, *48*, 8616−8639.

(3) Ge, Z.-H.; Zhao, L.-D.; Wu, D.; Liu, X.; Zhang, B.-P.; Li, J.-F.; He, J. Low-cost, abundant binary sulfides as promising thermoelectric materials. *Mater. Today* **2016**, *19*, 227−239.

(4) Banik, A.; Roychowdhury, S.; Biswas, K. The journey of tin chalcogenides towards high-performance thermoelectrics and topological materials. *Chem. Commun.* **2018**, *54*, 6573−6590.

(5) Chang, C.; Wu, M.; He, D.; Pei, Y.; Wu, C.-F.; Wu, X.; Yu, H.; Zhu, F.; Wang, K.; Chen, Y.; Huang, L.; Li, J.-F.; He, J.; Zhao, L.-D.

DOI: 10.1021/acs.chemmater.8b02676
Chem. Mater. 2018, 30, 5799−5813

3D charge and 2D phonon transports leading to high out-of-plane ZT in n-type SnSe crystals. *Science* **2018**, *360*, 778−783.
(6) Heremans, J. P.; Jovovic, V.; Toberer, E. S.; Saramat, A.; Kurosaki, K.; Charoenphakdee, A.; Yamanaka, S.; Snyder, G. J. Enhancement of Thermoelectric Efficiency in PbTe by Distortion of the Electronic Density of States. *Science* **2008**, *321*, 554−557.
(7) Zhang, Q.; Liao, B.; Lan, Y.; Lukas, K.; Liu, W.; Esfarjani, K.; Opeil, C.; Broido, D.; Chen, G.; Ren, Z. High thermoelectric performance by resonant dopant indium in nanostructured SnTe. *Proc. Natl. Acad. Sci. U. S. A.* **2013**, *110*, 13261−13266.
(8) Pei, Y.; Shi, X.; LaLonde, A.; Wang, H.; Chen, L.; Snyder, G. J. Convergence of electronic bands for high performance bulk thermoelectrics. *Nature* **2011**, *473*, 66−69.
(9) Zhao, L. D.; Wu, H. J.; Hao, S. Q.; Wu, C. I.; Zhou, X. Y.; Biswas, K.; He, J. Q.; Hogan, T. P.; Uher, C.; Wolverton, C.; Dravid, V. P.; Kanatzidis, M. G. All-scale hierarchical thermoelectrics: MgTe in PbTe facilitates valence band convergence and suppresses bipolar thermal transport for high performance. *Energy Environ. Sci.* **2013**, *6*, 3346−3355.
(10) Banik, A.; Shenoy, U. S.; Anand, S.; Waghmare, U. V.; Biswas, K. Mg Alloying in SnTe Facilitates Valence Band Convergence and Optimizes Thermoelectric Properties. *Chem. Mater.* **2015**, *27*, 581−587.
(11) Faleev, S. V.; Leonard, F. Theory of enhancement of thermoelectric properties of materials with nanoinclusions. *Phys. Rev. B: Condens. Matter Mater. Phys.* **2008**, *77*, 214304.
(12) Hicks, L. D.; Dresselhaus, M. S. Effect of quantum-well structures on the thermoelectric figure of merit. *Phys. Rev. B: Condens. Matter Mater. Phys.* **1993**, *47*, 12727−12731.
(13) Biswas, K.; He, J.; Blum, I. D.; Wu, C.-I.; Hogan, T. P.; Seidman, D. N.; Dravid, V. P.; Kanatzidis, M. G. High-performance bulk thermoelectrics with all-scale hierarchical architectures. *Nature* **2012**, *489*, 414−418.
(14) Biswas, K.; He, J.; Zhang, Q.; Wang, G.; Uher, C.; Dravid, V. P.; Kanatzidis, M. G. Strained endotaxial nanostructures with high thermoelectric figure of merit. *Nat. Chem.* **2011**, *3*, 160−166.
(15) Poudel, B.; Hao, Q.; Ma, Y.; Lan, Y.; Minnich, A.; Yu, B.; Yan, X.; Wang, D.; Muto, A.; Vashaee, D.; Chen, X.; Liu, J.; Dresselhaus, M. S.; Chen, G.; Ren, Z. High-Thermoelectric Performance of Nanostructured Bismuth Antimony Telluride Bulk Alloys. *Science* **2008**, *320*, 634−638.
(16) Samanta, M.; Biswas, K. Low Thermal Conductivity and High Thermoelectric Performance in $(GeTe)_{1-2x}(GeSe)_x(GeS)_x$: Competition between Solid Solution and Phase Separation. *J. Am. Chem. Soc.* **2017**, *139*, 9382−9391.
(17) Zhao, L.-D.; Dravid, V. P.; Kanatzidis, M. G. The panoscopic approach to high performance thermoelectrics. *Energy Environ. Sci.* **2014**, *7*, 251−268.
(18) Jana, M. K.; Biswas, K. Crystalline Solids with Intrinsically Low Lattice Thermal Conductivity for Thermoelectric Energy Conversion. *ACS Energy Lett.* **2018**, *3*, 1315−1324.
(19) Tan, G.; Shi, F.; Hao, S.; Zhao, L.-D.; Chi, H.; Zhang, X.; Uher, C.; Wolverton, C.; Dravid, V. P.; Kanatzidis, M. G. Non-equilibrium processing leads to record high thermoelectric figure of merit in PbTe-SrTe. *Nat. Commun.* **2016**, *7*, 12167.
(20) Perumal, S.; Roychowdhury, S.; Negi, D. S.; Datta, R.; Biswas, K. High Thermoelectric Performance and Enhanced Mechanical Stability of p-type $Ge_{1-x}Sb_xTe$. *Chem. Mater.* **2015**, *27*, 7171−7178.
(21) Rosi, F. D.; Dismukes, J. P.; Hockings, E. F. Semiconductor materials for thermoelectric power generation up to 700 C. *Electr. Eng.* **1960**, *79*, 450−459.
(22) Perumal, S.; Roychowdhury, S.; Biswas, K. High performance thermoelectric materials and devices based on GeTe. *J. Mater. Chem. C* **2016**, *4*, 7520−7536.
(23) Huang, Z.; Miller, S. A.; Ge, B.; Yan, M.; Anand, S.; Wu, T.; Nan, P.; Zhu, Y.; Zhuang, W.; Snyder, G. J.; Jiang, P.; Bao, X. High Thermoelectric Performance of New Rhombohedral Phase of GeSe stabilized through Alloying with $AgSbSe_2$. *Angew. Chem., Int. Ed.* **2017**, *56*, 14113−14118.
(24) Zhang, X.; Shen, J.; Lin, S.; Li, J.; Chen, Z.; Li, W.; Pei, Y. Thermoelectric properties of GeSe. *J. Materiomics* **2016**, *2*, 331−337.
(25) Hao, S.; Shi, F.; Dravid, V. P.; Kanatzidis, M. G.; Wolverton, C. Computational Prediction of High Thermoelectric Performance in Hole Doped Layered GeSe. *Chem. Mater.* **2016**, *28*, 3218−3226.
(26) Chattopadhyay, T.; Boucherle, J. X.; vonSchnering, H. G. Neutron diffraction study on the structural phase transition in GeTe. *J. Phys. C: Solid State Phys.* **1987**, *20*, 1431−1440.
(27) Steigmeier, E. F.; Harbeke, G. Soft phonon mode and ferroelectricity in GeTe. *Solid State Commun.* **1970**, *8*, 1275−1279.
(28) Andrikopoulos, K. S.; Yannopoulos, S. N.; Kolobov, A. V.; Fons, P.; Tominaga, J. Raman scattering study of GeTe and $Ge_2Sb_2Te_5$ phase-change materials. *J. Phys. Chem. Solids* **2007**, *68*, 1074−1078.
(29) Wdowik, U. D.; Parlinski, K.; Rols, S.; Chatterji, T. Soft-phonon mediated structural phase transition in GeTe. *Phys. Rev. B: Condens. Matter Mater. Phys.* **2014**, *89*, 224306.
(30) Perumal, S.; Roychowdhury, S.; Biswas, K. Reduction of thermal conductivity through nanostructuring enhances the thermoelectric figure of merit in $Ge_{1-x}Bi_xTe$. *Inorg. Chem. Front.* **2016**, *3*, 125−132.
(31) Wu, L.; Li, X.; Wang, S.; Zhang, T.; Yang, J.; Zhang, W.; Chen, L.; Yang, J. Resonant level-induced high thermoelectric response in indium-doped GeTe. *NPG Asia Mater.* **2017**, *9*, e343.
(32) Hong, M.; Chen, Z. G.; Yang, L.; Zou, Y. C.; Dargusch, M. S.; Wang, H.; Zou, J. Realizing zT of 2.3 in $Ge_{1-x-y}Sb_xIn_yTe$ via Reducing the Phase-Transition Temperature and Introducing Resonant Energy Doping. *Adv. Mater.* **2018**, *30*, 1705942.
(33) Perumal, S.; Bellare, P.; Shenoy, U. S.; Waghmare, U. V.; Biswas, K. Low Thermal Conductivity and High Thermoelectric Performance in Sb and Bi Codoped GeTe: Complementary Effect of Band Convergence and Nanostructuring. *Chem. Mater.* **2017**, *29*, 10426−10435.
(34) Chen, Y.; Jaworski, C. M.; Gao, Y. B.; Wang, H.; Zhu, T. J.; Snyder, G. J.; Heremans, J. P.; Zhao, X. B. Transport properties and valence band feature of high-performance $(GeTe)_{85}(AgSbTe_2)_{15}$ thermoelectric materials. *New J. Phys.* **2014**, *16*, 013057.
(35) Samanta, M.; Roychowdhury, S.; Ghatak, J.; Perumal, S.; Biswas, K. Ultrahigh Average Thermoelectric Figure of Merit, Low Lattice Thermal Conductivity and Enhanced Microhardness in Nanostructured $(GeTe)_x(AgSbSe_2)_{100-x}$. *Chem. - Eur. J.* **2017**, *23*, 7438−7443.
(36) Levin, E. M.; Cook, B. A.; Harringa, J. L.; Bud'ko, S. L.; Venkatasubramanian, R.; Schmidt-Rohr, K. Analysis of Ce-and Yb-Doped TAGS-85 Materials with Enhanced Thermoelectric Figure of Merit. *Adv. Funct. Mater.* **2011**, *21*, 441−447.
(37) Snyder, G. J.; Toberer, E. S. Complex thermoelectric materials. *Nat. Mater.* **2008**, *7* (2), 105−114.
(38) Gelbstein, Y.; Davidow, J.; Girard, S. N.; Chung, D. Y.; Kanatzidis, M. Controlling Metallurgical Phase Separation Reactions of the $Ge_{0.87}Pb_{0.13}Te$ Alloy for High Thermoelectric Performance. *Adv. Energy Mater.* **2013**, *3*, 815−820.
(39) Gelbstein, Y.; Davidow, J. Highly efficient functional $Ge_xPb_{1-x}Te$ based thermoelectric alloys. *Phys. Chem. Chem. Phys.* **2014**, *16*, 20120−20126.
(40) Wu, D.; Zhao, L.-D.; Hao, S.; Jiang, Q.; Zheng, F.; Doak, J. W.; Wu, H.; Chi, H.; Gelbstein, Y.; Uher, C.; Wolverton, C.; Kanatzidis, M.; He, J. Origin of the High Performance in GeTe-Based Thermoelectric Materials upon Bi_2Te_3 Doping. *J. Am. Chem. Soc.* **2014**, *136*, 11412−11419.
(41) Li, J.; Zhang, X.; Chen, Z.; Lin, S.; Li, W.; Shen, J.; Witting, I. T.; Faghaninia, A.; Chen, Y.; Jain, A.; Chen, L.; Snyder, G. J.; Pei, Y. Low-Symmetry Rhombohedral GeTe Thermoelectrics. *Joule* **2018**, *2*, 976−987.
(42) Roychowdhury, S.; Biswas, K. Slight Symmetry Reduction in Thermoelectrics. *Chem.* **2018**, *4*, 939−942.
(43) Zhao, L.-D.; Lo, S.-H.; Zhang, Y.; Sun, H.; Tan, G.; Uher, C.; Wolverton, C.; Dravid, V. P.; Kanatzidis, M. G. Ultralow thermal

DOI: 10.1021/acs.chemmater.8b02676
Chem. Mater. 2018, 30, 5799−5813

conductivity and high thermoelectric figure of merit in SnSe crystals. *Nature* **2014**, *508*, 373−377.
(44) Shaltaf, R.; Gonze, X.; Cardona, M.; Kremer, R. K.; Siegle, G. Lattice dynamics and specific heat of alpha-GeTe: Theoretical and experimental study. *Phys. Rev. B: Condens. Matter Mater. Phys.* **2009**, *79*, 075204.
(45) Rabe, K. M.; Joannopoulos, J. D. Ab initio determination of a structural phase transition temperature. *Phys. Rev. Lett.* **1987**, *59*, 570−573.
(46) Rabe, K. M.; Joannopoulos, J. D. Theory of the structural phase transition of GeTe. *Phys. Rev. B: Condens. Matter Mater. Phys.* **1987**, *36*, 6631−6639.
(47) Zeier, W. G.; Zevalkink, A.; Gibbs, Z. M.; Hautier, G.; Kanatzidis, M. G.; Snyder, G. J. Thinking like a chemist: intuition in thermoelectric materials. *Angew. Chem., Int. Ed.* **2016**, *55*, 6826−6841.
(48) Waghmare, U. V.; Spaldin, N. A.; Kandpal, H. C.; Seshadri, R. First-principles indicators of metallicity and cation off-centricity in the IV-VI rocksalt chalcogenides of divalent Ge, Sn, and Pb. *Phys. Rev. B: Condens. Matter Mater. Phys.* **2003**, *67*, 125111.
(49) Shaltaf, R.; Durgun, E.; Raty, J. Y.; Ghosez, P.; Gonze, X. Dynamical, dielectric, and elastic properties of GeTe investigated with first-principles density functional theory. *Phys. Rev. B: Condens. Matter Mater. Phys.* **2008**, *78*, 205203.
(50) Aggarwal, L.; Banik, A.; Anand, S.; Waghmare, U. V.; Biswas, K.; Sheet, G. Local ferroelectricity in thermoelectric SnTe above room temperature driven by competing phonon instabilities and soft resonant bonding. *J. Materiomics* **2016**, *2*, 196−202.
(51) Murphy, R. M.; Murray, Ã. a. D.; Fahy, S.; Savić, I. Ferroelectric phase transition and the lattice thermal conductivity of $Pb_{1-x}Ge_xTe$ alloys. *Phys. Rev. B: Condens. Matter Mater. Phys.* **2017**, *95*, 144302.
(52) Daughton, W. J.; DeFacio, D. Lattice instability and phonon-widths in $Pb_{1-x}Sn_xTe$. *J. Phys. C: Solid State Phys.* **1978**, *11*, 4307.
(53) Matsunaga, T.; Fons, P.; Kolobov, A. V.; Tominaga, J.; Yamada, N. The order-disorder transition in GeTe: Views from different length-scales. *Appl. Phys. Lett.* **2011**, *99*, 231907.
(54) Fons, P.; Kolobov, A. V.; Krbal, M.; Tominaga, J.; Andrikopoulos, K. S.; Yannopoulos, S. N.; Voyiatzis, G. A.; Uruga, T. Phase transition in crystalline GeTe: Pitfalls of averaging effects. *Phys. Rev. B: Condens. Matter Mater. Phys.* **2010**, *82*, 155209.
(55) Ovshinsky, S. R. Reversible Electrical Switching Phenomena in Disordered Structures. *Phys. Rev. Lett.* **1968**, *21*, 1450−1453.
(56) Libera, M.; Chen, M. Time-resolved reflection and transmission studies of amorphous Ge-Te thin-film crystallization. *J. Appl. Phys.* **1993**, *73*, 2272−2282.
(57) Chatterji, T.; Kumar, C. M. N.; Wdowik, U. D. Anomalous temperature-induced volume contraction in GeTe. *Phys. Rev. B: Condens. Matter Mater. Phys.* **2015**, *91*, 054110.
(58) Sun, Z.; Zhou, J.; Mao, H.-K.; Ahuja, R. Peierls distortion mediated reversible phase transition in GeTe under pressure. *Proc. Natl. Acad. Sci. U. S. A.* **2012**, *109*, 5948−5952.
(59) Bauer Pereira, P.; Sergueev, I.; Gorsse, S.; Dadda, J.; Muller, E.; Hermann, R. P. Lattice dynamics and structure of GeTe, SnTe and PbTe. *Phys. Status Solidi B* **2013**, *250*, 1300−1307.
(60) Lee, S.; Esfarjani, K.; Luo, T.; Zhou, J.; Tian, Z.; Chen, G. Resonant bonding leads to low lattice thermal conductivity. *Nat. Commun.* **2014**, *5*, 3525.
(61) Cai, X.; Wei, J. Temperature dependence of the thermal properties of InSb materials used in data storage. *J. Appl. Phys.* **2013**, *114*, 083507.
(62) Zhou, X.; Yan, Y.; Lu, X.; Zhu, H.; Han, X.; Chen, G.; Ren, Z. Routes for high-performance thermoelectric materials. *Mater. Today* **2018**, DOI: 10.1016/j.mattod.2018.03.039.
(63) Sitter, H.; Lischka, K.; Heinrich, H. Structure of the second valence band in PbTe. *Phys. Rev. B* **1977**, *16*, 680−687.
(64) Allgaier, R. S. Valence Bands in Lead Telluride. *J. Appl. Phys.* **1961**, *32*, 2185−2189.
(65) Rogers, L. M. Valence band structure of SnTe. *J. Phys. D: Appl. Phys.* **1968**, *1*, 845−852.
(66) Santhanam, S.; Chaudhuri, A. K. Transport properties of SnTe interpreted by means of a two valence band model. *Mater. Res. Bull.* **1981**, *16*, 911−917.
(67) Pei, Y.; Wang, H.; Gibbs, Z. M.; LaLonde, A. D.; Snyder, G. J. Thermopower enhancement in $Pb_{1-x}Mn_xTe$ alloys and its effect on thermoelectric efficiency. *NPG Asia Mater.* **2012**, *4*, e28.
(68) Li, J.; Zhang, X.; Lin, S.; Chen, Z.; Pei, Y. Realizing the High Thermoelectric Performance of GeTe by Sb-Doping and Se-Alloying. *Chem. Mater.* **2017**, *29*, 605−611.
(69) Liu, Z.; Sun, J.; Mao, J.; Zhu, H.; Ren, W.; Zhou, J.; Wang, Z.; Singh, D. J.; Sui, J.; Chu, C.-W.; Ren, Z. Phase-transition temperature suppression to achieve cubic GeTe and high thermoelectric performance by Bi and Mn codoping. *Proc. Natl. Acad. Sci. U. S. A.* **2018**, *115*, 5332−5337.
(70) Lewis, J. E. The Defect Structure of Non-Stoichiometric Germanium Telluride from Magnetic Susceptibility Measurements. *Phys. Status Solidi B* **1970**, *38*, 131−140.
(71) Lewis, J. E. Optical properties and energy gap of GeTe from reflectance studies. *Phys. Status Solidi B* **1973**, *59*, 367−377.
(72) Korzhuev, M. A. On the Fundamental Energy Gap in GeTe. *Phys. Status Solidi B* **1982**, *112*, 39−41.
(73) Zheng, Z.; Su, X.; Deng, R.; Stoumpos, C.; Xie, H.; Liu, W.; Yan, Y.; Hao, S.; Uher, C.; Wolverton, C.; Kanatzidis, M. G.; Tang, X. Rhombohedral to Cubic Conversion of GeTe via MnTe Alloying Leads to Ultralow Thermal Conductivity, Electronic Band Convergence, and High Thermoelectric Performance. *J. Am. Chem. Soc.* **2018**, *140*, 2673−2686.
(74) Pei, Y.; LaLonde, A.; Iwanaga, S.; Snyder, G. J. High thermoelectric figure of merit in heavy hole dominated PbTe. *Energy Environ. Sci.* **2011**, *4*, 2085−2089.
(75) Zhou, M.; Gibbs, Z. M.; Wang, H.; Han, Y.; Xin, C.; Li, L.; Snyder, G. J. Optimization of thermoelectric efficiency in SnTe: the case for the light band. *Phys. Chem. Chem. Phys.* **2014**, *16*, 20741−20748.
(76) Li, J.; Chen, Z.; Zhang, X.; Sun, Y.; Yang, J.; Pei, Y. Electronic origin of the high thermoelectric performance of GeTe among the p-type group IV monotellurides. *NPG Asia Mater.* **2017**, *9*, e353.
(77) Mott, N. F.; Davis, E. A. *Electronic Processes in Non-Crystalline Materials*; Oxford University Press: Oxford, UK, 1971.
(78) Zhang, Q.; Wang, H.; Liu, W.; Wang, H.; Yu, B.; Zhang, Q.; Tian, Z.; Ni, G.; Lee, S.; Esfarjani, K.; Chen, G.; Ren, Z. Enhancement of thermoelectric figure-of-merit by resonant states of aluminium doping in lead selenide. *Energy Environ. Sci.* **2012**, *5*, 5246−5251.
(79) Chen, Z.; Zhang, X.; Pei, Y. Manipulation of Phonon Transport in Thermoelectrics. *Adv. Mater.* **2018**, *30*, 1705617.
(80) Daniels, L. M.; Savvin, S. N.; Pitcher, M. J.; Dyer, M. S.; Claridge, J. B.; Ling, S.; Slater, B.; Cora, F.; Alaria, J.; Rosseinsky, M. J. Phonon-glass electron-crystal behaviour by A site disorder in n-type thermoelectric oxides. *Energy Environ. Sci.* **2017**, *10*, 1917−1922.
(81) Lee, J. K.; Oh, M. W.; Kim, B. S.; Min, B. K.; Lee, H. W.; Park, S. D. Influence of Mn on crystal structure and thermoelectric properties of GeTe compounds. *Electron. Mater. Lett.* **2014**, *10*, 813−817.
(82) Li, J.; Chen, Z.; Zhang, X.; Yu, H.; Wu, Z.; Xie, H.; Chen, Y.; Pei, Y. Simultaneous Optimization of Carrier Concentration and Alloy Scattering for Ultrahigh Performance GeTe Thermoelectrics. *Adv. Sci.* **2017**, *4*, 1700341.
(83) Korkosz, R. J.; Chasapis, T. C.; Lo, S.-h.; Doak, J. W.; Kim, Y. J.; Wu, C.-I.; Hatzikraniotis, E.; Hogan, T. P.; Seidman, D. N.; Wolverton, C.; Dravid, V. P.; Kanatzidis, M. G. High ZT in *p*-Type $(PbTe)_{1-2x}(PbSe)_x(PbS)_x$ Thermoelectric Materials. *J. Am. Chem. Soc.* **2014**, *136*, 3225−3237.
(84) Davidow, J.; Gelbstein, Y. A Comparison Between the Mechanical and Thermoelectric Properties of Three Highly Efficient *p*-Type GeTe-Rich Compositions: TAGS-80, TAGS-85, and 3% Bi_2Te_3-Doped $Ge_{0.87}Pb_{0.13}Te$. *J. Electron. Mater.* **2013**, *42*, 1542−1549.
(85) Schroder, T.; Rosenthal, T.; Giesbrecht, N.; Nentwig, M.; Maier, S.; Wang, H.; Snyder, G. J.; Oeckler, O. Nanostructures in Te/

DOI: 10.1021/acs.chemmater.8b02676
Chem. Mater. 2018, 30, 5799−5813

Sb/Ge/Ag (TAGS) Thermoelectric Materials Induced by Phase Transitions Associated with Vacancy Ordering. *Inorg. Chem.* **2014**, *53*, 7722−7729.
(86) Yang, S. H.; Zhu, T. J.; Sun, T.; He, J.; Zhang, S. N.; Zhao, X. B. Nanostructures in high-performance $(GeTe)_x(AgSbTe_2)_{100-x}$ thermoelectric materials. *Nanotechnology* **2008**, *19*, 245707.
(87) Gorsse, S.; Bauer Pereira, P.; Decourt, R.; Sellier, E. Microstructure Engineering Design for Thermoelectric Materials: An Approach to Minimize Thermal Diffusivity. *Chem. Mater.* **2010**, *22*, 988−993.
(88) Fahrnbauer, F.; Souchay, D.; Wagner, G.; Oeckler, O. High Thermoelectric Figure of Merit Values of Germanium Antimony Tellurides with Kinetically Stable Cobalt Germanide Precipitates. *J. Am. Chem. Soc.* **2015**, *137*, 12633−12638.
(89) Zhao, L.-D.; Tan, G.; Hao, S.; He, J.; Pei, Y.; Chi, H.; Wang, H.; Gong, S.; Xu, H.; Dravid, V. P.; Uher, C.; Snyder, G. J.; Wolverton, C.; Kanatzidis, M. G. Ultrahigh power factor and thermoelectric performance in hole-doped single-crystal SnSe. *Science* **2016**, *351*, 141−144.
(90) Wei, T.-R.; Tan, G.; Zhang, X.; Wu, C.-F.; Li, J.-F.; Dravid, V. P.; Snyder, G. J.; Kanatzidis, M. G. Distinct Impact of Alkali-Ion Doping on Electrical Transport Properties of Thermoelectric p-Type Polycrystalline SnSe. *J. Am. Chem. Soc.* **2016**, *138*, 8875−8882.
(91) Deringer, V. L.; Stoffel, R. P.; Dronskowski, R. Vibrational and thermodynamic properties of GeSe in the quasiharmonic approximation. *Phys. Rev. B: Condens. Matter Mater. Phys.* **2014**, *89*, 094303.
(92) Yan, M.; Tan, X.; Huang, Z.; Liu, G.; Jiang, P.; Bao, X. Synergetic optimization of electronic and thermal transport for high-performance thermoelectric GeSe-$AgSbTe_2$ alloy. *J. Mater. Chem. A* **2018**, *6*, 8215−8220.
(93) von Rohr, F. O.; Ji, H.; Cevallos, F. A.; Gao, T.; Ong, N. P.; Cava, R. J. High-Pressure Synthesis and Characterization of β-GeSe - A Six-Membered-Ring Semiconductor in an Uncommon Boat Conformation. *J. Am. Chem. Soc.* **2017**, *139*, 2771−2777.
(94) Yang, K.; Setyawan, W.; Wang, S.; Buongiorno Nardelli, M.; Curtarolo, S. A search model for topological insulators with high-throughput robustness descriptors. *Nat. Mater.* **2012**, *11*, 614−619.
(95) Schroder, T.; Schneider, M. N.; Rosenthal, T.; Eisele, A.; Gold, C.; Scheidt, E.-W.; Scherer, W.; Berthold, R.; Oeckler, O. Nanostructures in metastable $GeBi_2Te_4$ obtained by high-pressure synthesis and rapid quenching and their influence on physical properties. *Phys. Rev. B: Condens. Matter Mater. Phys.* **2011**, *84*, 184104.
(96) Hazan, E.; Ben-Yehuda, O.; Madar, N.; Gelbstein, Y. Functional Graded Germanium-Lead Chalcogenide-Based Thermoelectric Module for Renewable Energy Applications. *Adv. Energy Mater.* **2015**, *5*, 1500272.

DOI: 10.1021/acs.chemmater.8b02676
Chem. Mater. 2018, 30, 5799−5813